AD-A041 317 TIMKEN CO CANTON OHIO F/G 21/5

TAPERED ROLLER BEARING DEVELOPMENT FOR AIRCRAFT TURBINE ENGINES--ETC(U)

APR 77 P S ORVOS F33615-76-C-2019

UNCLASSIFIED AFAPL-TR-77-6 NL

1 OF 1
ADA
041317

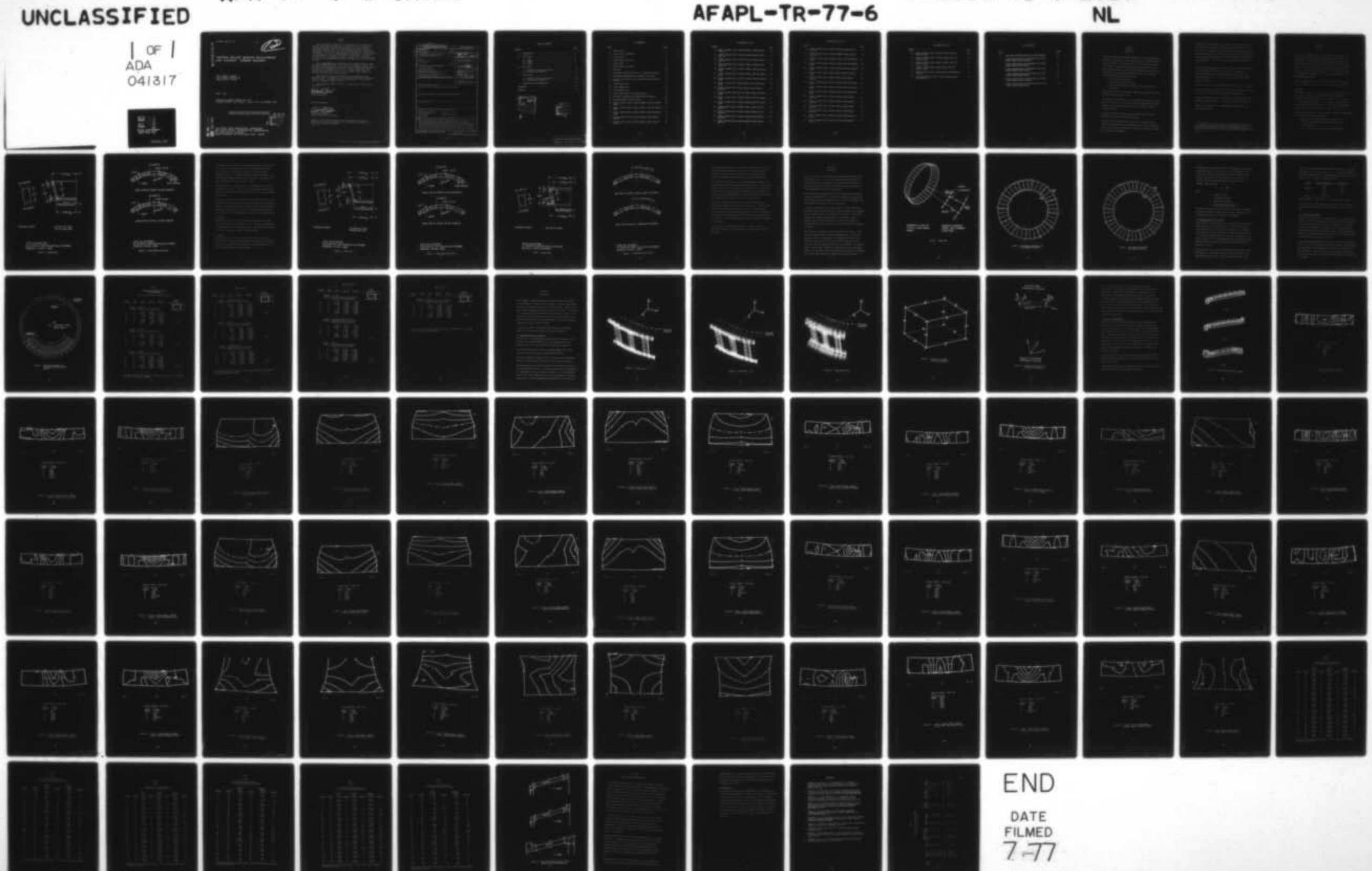

END

DATE
FILMED
7-77

1·0 2·8 2·5 5·0 3·15 2·2 5·6 6·3 3·5 2·0 1·1 7·1 4·0 4·5 1·8 1·25 1·4 1·6

NATIONAL BUREAU OF STANDARDS
MICROCOPY RESOLUTION TEST CHART

AFAPL-TR-77-6

12

ADA041317

TAPERED ROLLER BEARING DEVELOPMENT FOR AIRCRAFT TURBINE ENGINES

THE TIMKEN COMPANY
1835 DUEBER AVENUE SW
CANTON, OHIO 44706

APRIL 1977

TECHNICAL REPORT AFAPL-TR-77-6
INTERIM REPORT FOR PERIOD MARCH 1976 — DECEMBER 1976

Approved for public release; distribution unlimited

AIR FORCE AERO PROPULSION LABORATORY
AIR FORCE WRIGHT AERONAUTICAL LABORATORIES
Air Force Systems Command
Wright-Patterson Air Force Base, Ohio 45433

NOTICE

When Government drawings, specifications, or other data are used for any purpose other than in connection with a definitely related Government procurement operation, the United States Government thereby incurs no responsibility nor any obligation whatsoever; and the fact that the Government may have formulated, furnished, or in any way supplied the said drawings, specifications, or other data, is not to be regarded by implication or otherwise as in any manner licensing the holder or any other person or corporation, or conveying any rights or permission to manufacture, use, or sell any patented invention that may in any way be related thereto.

This final report was submitted by The Timken Company, under Contract F33615-76-C-2019. The effort was sponsored by the Air Force Aero-Propulsion Laboratory, Air Force Systems Command, Wright-Patterson Air Force Base, Ohio under Project 3048, Task 304806, and Work Unit 30480684, with Lt. R. L. Gissel (AFAPL/SFL) as project engineer. Mr. Peter S. Orvos of The Timken Company was technically responsible for the work.

This report has been reviewed by the Information Office (ASD/OIP), and is releasable to the National Technical Information Service (NTIS). At NTIS, it will be available to the general public, including foreign nations.

This technical report has been reviewed and is approved for publication.

Richard L. Gissel

Lt. R. L. Gissel
Project Engineer

FOR THE COMMANDER

Howard F. Jones

HOWARD F. JONES, Chief
Lubrication Branch
Fuels & Lubrication Division

Copies of this report should not be returned unless return is required by security considerations, contractual obligations, or notice on a specific document.

UNCLASSIFIED

SECURITY CLASSIFICATION OF THIS PAGE (When Data Entered)

REPORT DOCUMENTATION PAGE

READ INSTRUCTIONS BEFORE COMPLETING FORM

1. REPORT NUMBER: AFAPL-TR-77-6	2. GOVT ACCESSION NO.
3. RECIPIENT'S CATALOG NUMBER	
4. TITLE (and Subtitle): TAPERED ROLLER BEARING DEVELOPMENT FOR AIRCRAFT TURBINE ENGINES.	5. TYPE OF REPORT & PERIOD COVERED: ~~INTERIM~~ FINA[L] REPORT. 8 March 1976-8 January 1977
	6. PERFORMING ORG. REPORT NUMBER
7. AUTHOR(s): Peter S. Orvos	8. CONTRACT OR GRANT NUMBER(s): F33615-76-C-2019
9. PERFORMING ORGANIZATION NAME AND ADDRESS: The Timken Company, 1835 Dueber Avenue, S.W., Canton, Ohio 44706	10. PROGRAM ELEMENT, PROJECT, TASK AREA & WORK UNIT NUMBERS: Project No. 3048; Task No. 304806; Work Unit No. 30480684
11. CONTROLLING OFFICE NAME AND ADDRESS: Air Force Aero Propulsion Laboratory/SFL, Air Force Systems Command, Wright-Patterson Air Force Base, Ohio 45433	12. REPORT DATE: 11 Apr 77
	13. NUMBER OF PAGES: 91 (92p.)
14. MONITORING AGENCY NAME & ADDRESS (if different from Controlling Office)	15. SECURITY CLASS. (of this report): UNCLASSIFIED
	15a. DECLASSIFICATION/DOWNGRADING SCHEDULE

16. DISTRIBUTION STATEMENT (of this Report)

Approved for public release; distribution unlimited.

17. DISTRIBUTION STATEMENT (of the abstract entered in Block 20, if different from Report)

18. SUPPLEMENTARY NOTES

19. KEY WORDS (Continue on reverse side if necessary and identify by block number)

- Tapered Roller Bearings
- Finite Element Analysis
- Stress Analysis
- Cage Design
- Centrifugal Force
- Deformation
- Mechanical Properties

20. ABSTRACT (Continue on reverse side if necessary and identify by block number)

Finite element methods were used to structurally analyze various potential high speed tapered roller bearing cage designs. These cage designs included roller guided and race guided configurations. The two approaches used in the analysis were first to model the full cage using beam elements and then intensively analyze a segment using solid elements. In summary it was determined that centrifugal forces mostly affect high speed cage stress and deformation, and the race guided cage exhibits the greatest strength.

DD FORM 1 JAN 73 1473 EDITION OF 1 NOV 65 IS OBSOLETE

UNCLASSIFIED

SECURITY CLASSIFICATION OF THIS PAGE (When Data Entered)

408393

TABLE OF CONTENTS

ILLUSTRATIONS

ILLUSTRATIONS (Con't.)

ILLUSTRATIONS (Con't.)

LIST OF TABLES

SECTION I

INTRODUCTION

A prior investigation by The Timken Company (ref. 1) has demonstrated the feasibility of operating a tapered roller bearing in an aircraft turbine engine environment. In this program 4.25 in. (107.95 mm) bore bearings were tested to 3.5 million DN under thrust loads ranging to 5000 lbf. These tests were conducted using a modified stamped low carbon steel cage currently used in conventional tapered roller bearings. The design modifications investigated were as follows:

a. Silver plating the surface
b. Carburizing for greater strength
c. Extending and notching the large end flange for cage speed measurements

Note: The term 'cage' is the bearing component that separates the rollers and retains them as a unit to a race.

The test results revealed that after a short period of operation, ranging from 1 to 15.5 hours at 3.5 million DN, the cage would plastically deform, fracture at the large end-bridge intersection and damage the bearing contacting surfaces.

At a reduced speed of 3 million DN a cage survived 147 hours prior to deformation, fracture and bearing surface damage.

Estimates of cage tangential stresses done prior to conducting these tests had indicated that inertia induced stresses would be at the material elastic limit. Therefore, when plastic deformation and fracture occurred, the results were not unexpected.

The objective of this program is to enhance the state-of-the-art of high speed tapered roller bearings. The approach will be in two phases. The first being the development of a cage that is able to operate successfully under high speed conditions. The second phase being the further definition of bearing performance capabilities in the environment of current turbine engine mainshaft. This phase will focus on heat generation and fatigue life.

This interim report presents the results of structural analysis performed on various potential high speed cage designs.[1] The analysis was accomplished using Structural Dynamics Research Corporation's computer program SUPERB Version 4.0. It is based on the finite element method of structural analysis.

Section II presents the various cage designs and materials to be analyzed.

Section III covers the finite element studies conducted on the complete cage. In this approach, space beams were used as the modeling element.

Segments of three cage designs were modeled using solid elements having a parabolic displacement order. These results are presented in Section IV.

Section V is the conclusions and recommendations derived from these finite element studies.

---

[1]There have been numerous analytical and experimental investigations toward predicting cage motion. These studies (references 2, 3, 4, 5, 6 and 7) have concentrated on roller/ball slip (deviation from epicyclic motion), whereas, this effort considers only the structural aspects of the cage.

SECTION II

CAGE DESIGNS

Inherent space limitations within a tapered roller bearing limit the potential cage designs. These are further limited by the criteria of a maximum number of rollers to yield the greatest bearing capacity. The primary functions of the cage are to separate the rollers and retain them as a unit to either race. In performing these functions the cage must: not restrict lubricant flow to the roller-race or roller end-rib conjunctions, minimize its contribution to heat (torque) generation and should be reasonable to manufacture.

The three designs analyzed in this investigation are identified as the 'L-cage,' 'S-cage' and 'Z-cage.' Discussions of these designs follow.

2.1 L-Cage

This design is illustrated in Figures 1 and 2. With modifications it was used in all tests of the previous AFAPL sponsored Timken Company investigation of high speed tapered roller bearings (ref. 1). The cage is a roller guided design; that is, it is completely guided and propelled by the rollers and does not interact with either race. The roller-cage conjunction is at the center of the wing surface. Refer to Figure 2.

This cage would be termed a conventional design. Its geometry established by a few simple relationships, for example:

a. Percent of roller diameter projection through cage O.D.

b. Minimum clearance between cage and cup (outer race) and cone (inner race)

c. Ratio of cage stock thickness to small end-bridge width

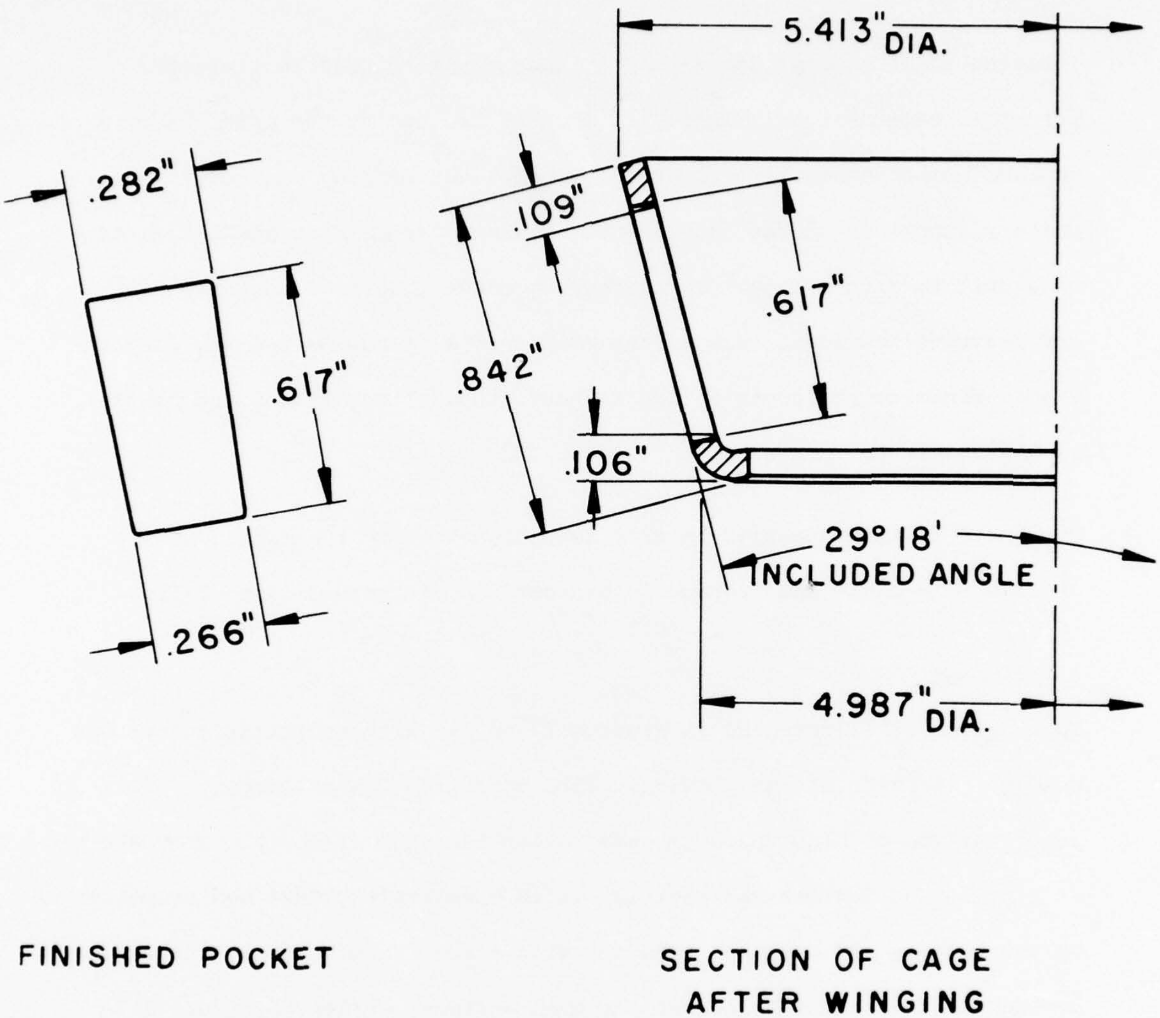

CAGE No. XC1933AB
39 POCKETS FOR ROLLER No. XC1933BC
NOMINAL STOCK = .065"

Figure 1 - L-Cage Design

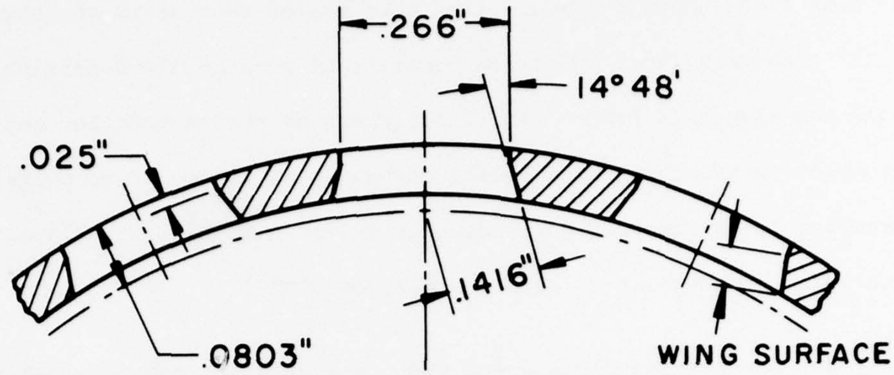

SMALL END OF POCKET AFTER WINGING

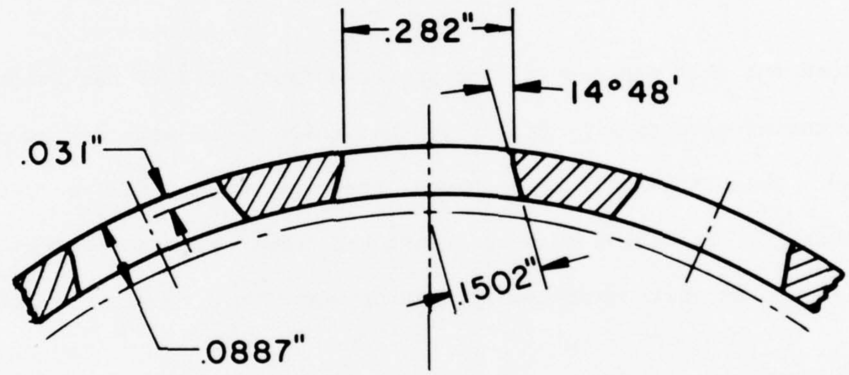

LARGE END OF POCKET AFTER WINGING

CAGE No. XC1933AB
39 POCKETS FOR ROLLER No. XC1933BC
NOMINAL STOCK = .065"

Figure 2 - L-Cage Bridge Cross-Section

The dimensions shown in Figure 1 of this design represents the cage prior to "closing-in." This operation consists of plastically deforming the small end flange to reduce radial looseness of the cage/roller set assembled on the cone. The radial looseness is called "cage shake." This parameter being measured perpendicular to the bridge at its midpoint. For high speed bearings it is held to .002" to .006".

The previous tests were conducted with this cage stamped from hot rolled SAE 1008-1010 sheet steel. Tensile tests on a sample of this sheet stock revealed it to have a yield strength of 32,000 psi and an ultimate strength of 42,000 psi.

The cages for this program will be produced from SAE 4340 bar stock. The manufacturing process will differ in that these cages will not be completely stamped. The blanks will be machined, then the pockets will be perforated individually. Providing that no cracks are formed in manufacture, these cages should exhibit considerably greater resistance to plastic deformation.

2.2 S-Cage

The S-Cage is identical to the L design with the exception of the large end-flange configuration (see Figures 3 and 4). The flange is extended and curved perpendicular to the bearing centerline. This modification increases the critical flange cross-sectional area by 57 percent.

2.3 Z-Cage

The race guided type of cage is presented in this design. Refer to Figures 5 and 6. Guidance for concentric rotation relative to the bearing centerline is provided by the cone large rib O.D. and an extension of the cup at the small end toward the bearing apex.

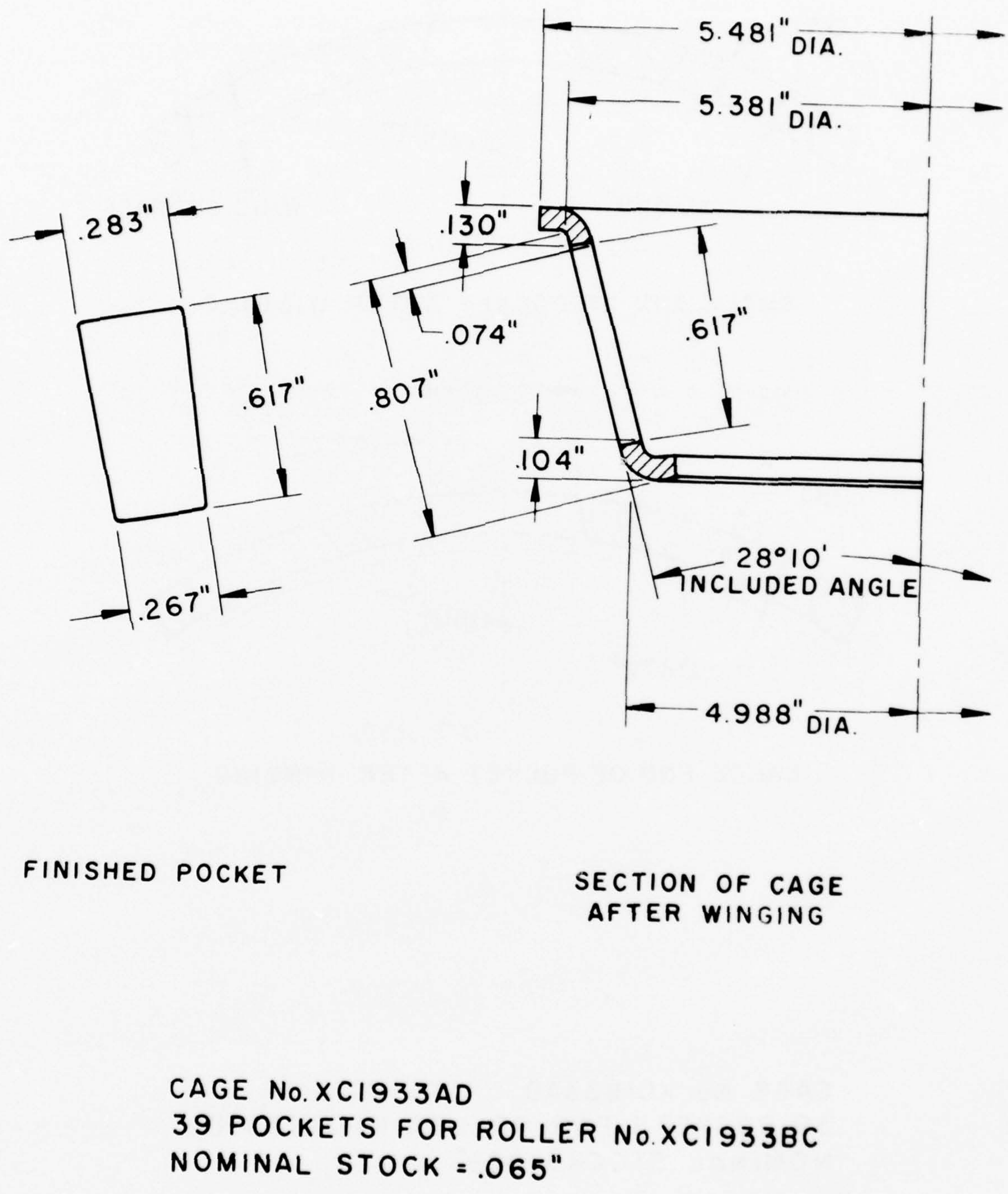

Figure 3 - S-Cage Design

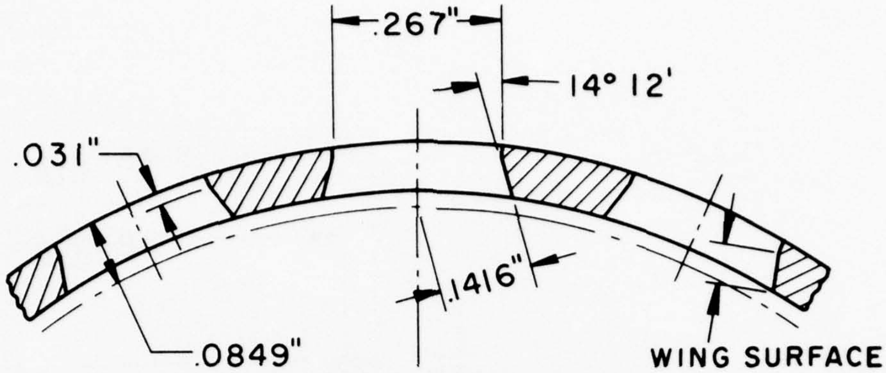

SMALL END OF POCKET AFTER WINGING

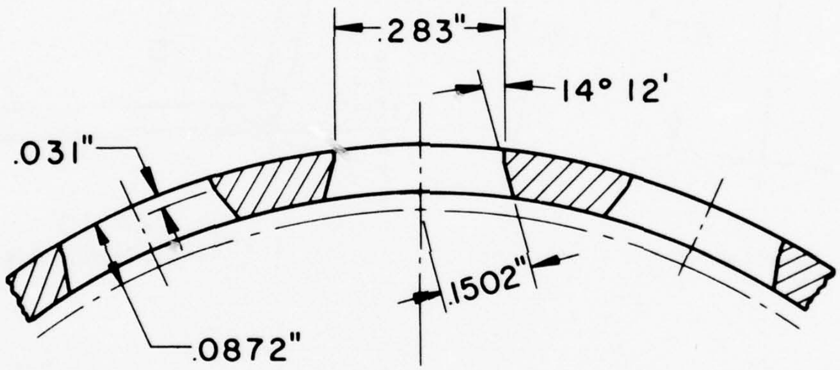

LARGE END OF POCKET AFTER WINGING

CAGE No. XC1933AD
39 POCKETS FOR ROLLER No. XC1933BC
NOMINAL STOCK = .065"

Figure 4 - S-Cage Bridge Cross-Section

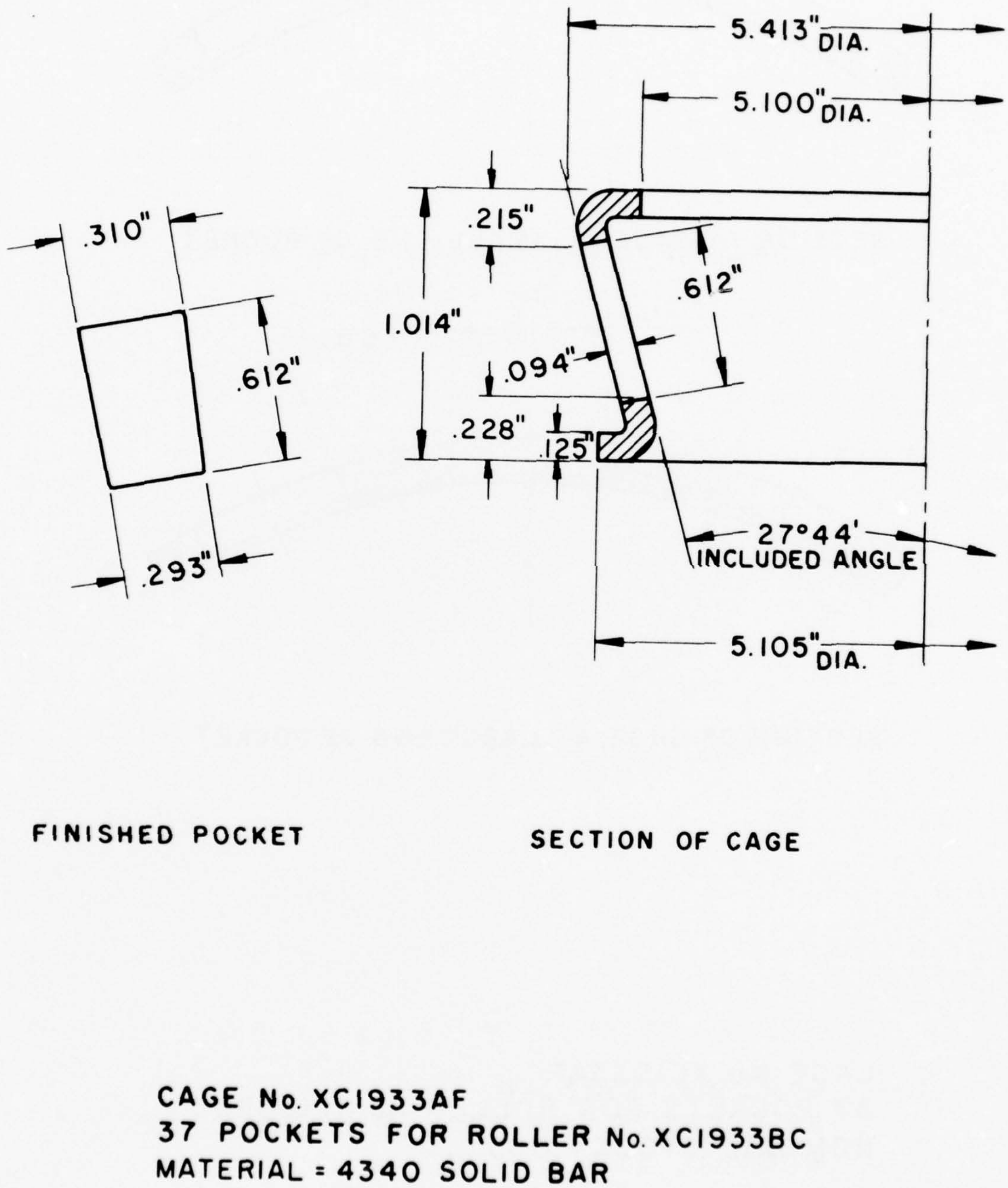

Figure 5 - Z-Cage Design

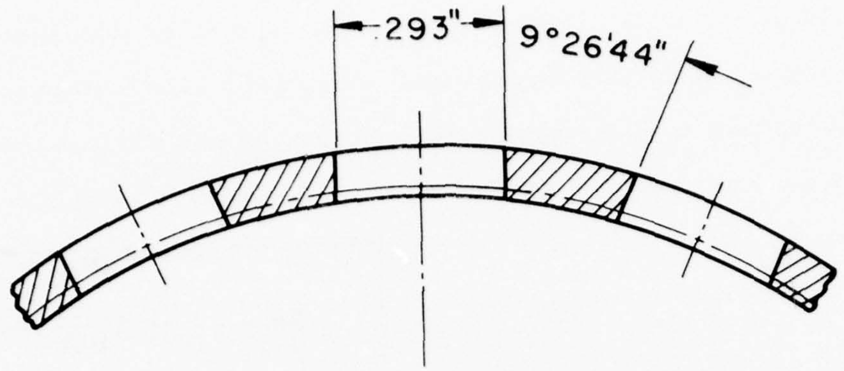

SECTION OF CAGE AT SMALL END OF POCKET

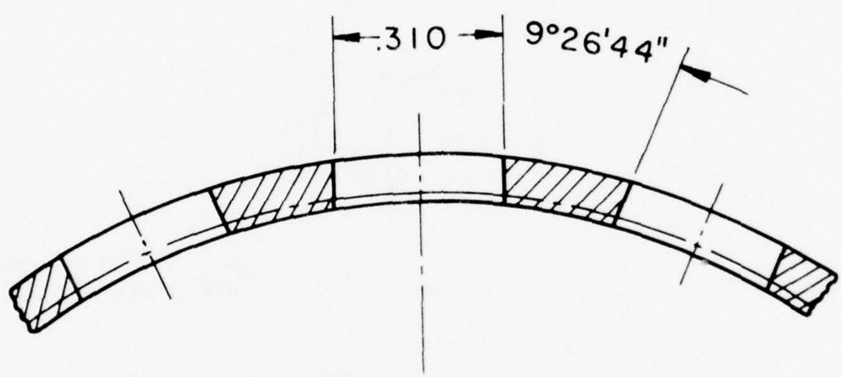

SECTION OF CAGE AT LARGE END OF POCKET

CAGE No. XC1933AF
37 POCKETS FOR ROLLER No. XC1933BC
NOMINAL STOCK = .065"

Figure 6 - Z-Cage Bridge Cross-Section

This scheme was selected to allow lubricant to be jetted to the small end of the roller without obstruction. The pilot at the large end tends to restrict the lubricant flow being pumped out of the bearing. This restriction should provide improved roller end-cone rib lubrication.

The cage-roller body conjunction is at the maximum roller diameter. The pocket width being .010" greater than the roller diameter. To unitize the rollers to the cone, slots are machined in each bridge O.D., then the thin wall sections are deformed plastically toward the roller centerline. By contacting at this maximum diameter, the number of rollers in the bearing are reduced from 39 in the L or S-cage to 37 for the Z-cage.

In rotating shaft applications, the angular velocity of the cage is approximately one-half the cone speed (epicyclic motion). Relative motion exists between the cage and its guiding surfaces. To operate without scoring or welding requires a hydrodynamic lubricant film. Calculations on the magnitude of the torque generated by shearing this film is presented in reference 1. These guides generate heat which is considered a detriment to this design.

The cage will be completely machined due to its thicker sections, dimensional tolerances and complex geometry. Material will be SAE 4340 bar stock.

SECTION III

BEAM MODELS

Structural analysis of the complete cage was accomplished using SDRC space beam elements (ref. 8). These provide an economical and accurate tool for analyzing general space frames. The element includes the effect of shear deformation and is capable of accurately studying cross sections that are nonsymmetric about the principal axes.

The three cage designs presented in Section II were modeled and analyzed under two loading conditions. In addition the L-design was geometrically and materially altered for parametric study. A total of ten computer runs were performed in this portion of the investigation.

The approach used in any finite element study "is to solve a structural problem by simulating a structure using a network of small pieces (elements) of known (defined) behaviors (stiffness)," from reference 9. The array of elements used to model the complete cage is illustrated in Figure 7. Numerical node and element designations for both L and S designs (39 roller pockets) are shown in Figure 8. The 37 pocket Z-design is depicted in Figure 9.

Each cage design is composed of three finite beam cross sections. These being the large-end flange, bridge and small-end flange. For the L and S design the bridge is a tapered beam. The assumption used is that this member had a constant cross section over its full length equal to the small-end. This would add negligible error to the analysis. For the beam models to have the same stress-strain characteristics of the actual cage design, it is necessary to define orientation and cross-sectional properties. For computing these properties the beam x-axis is located along the

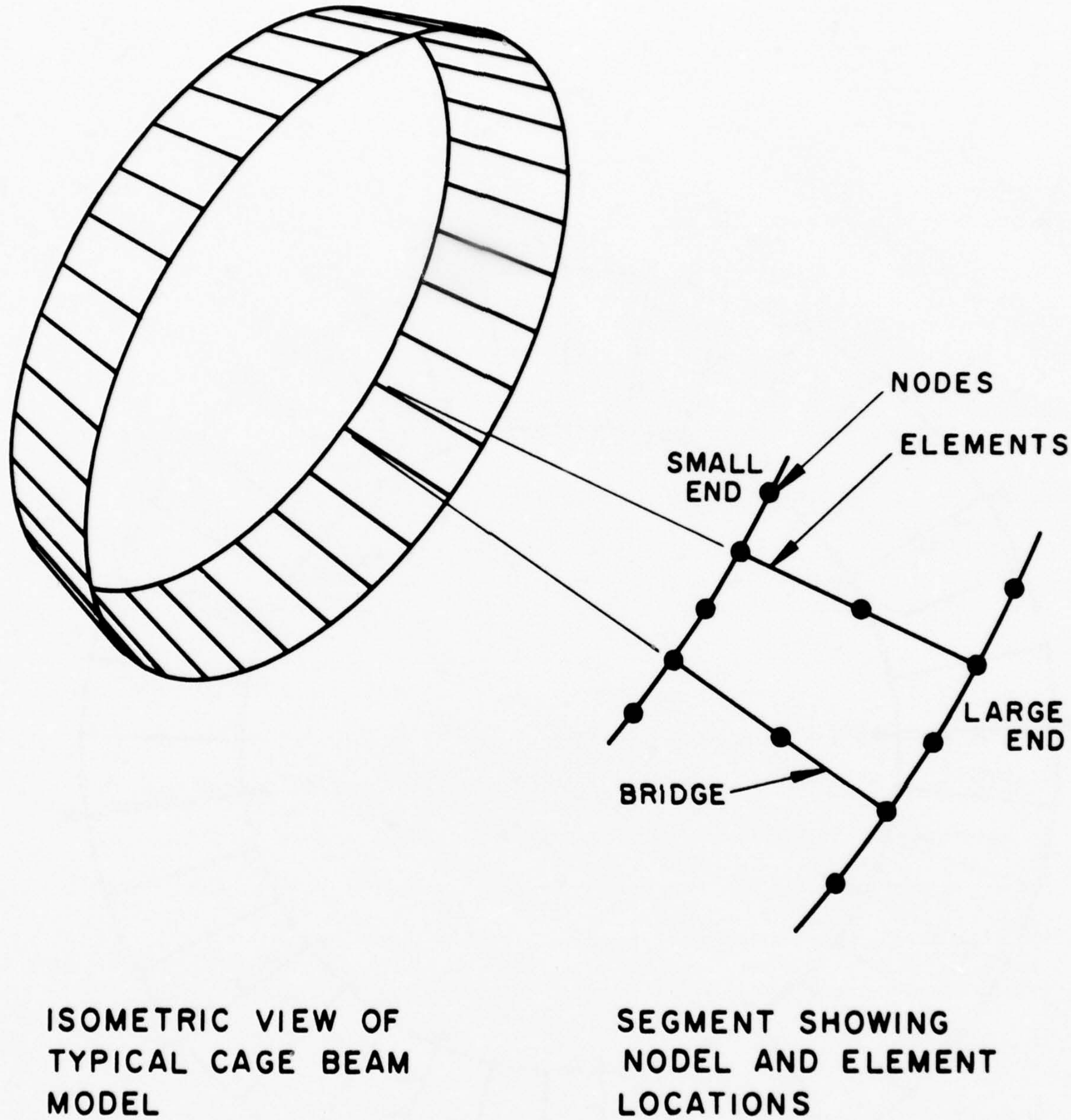

Figure 7 - Beam Model

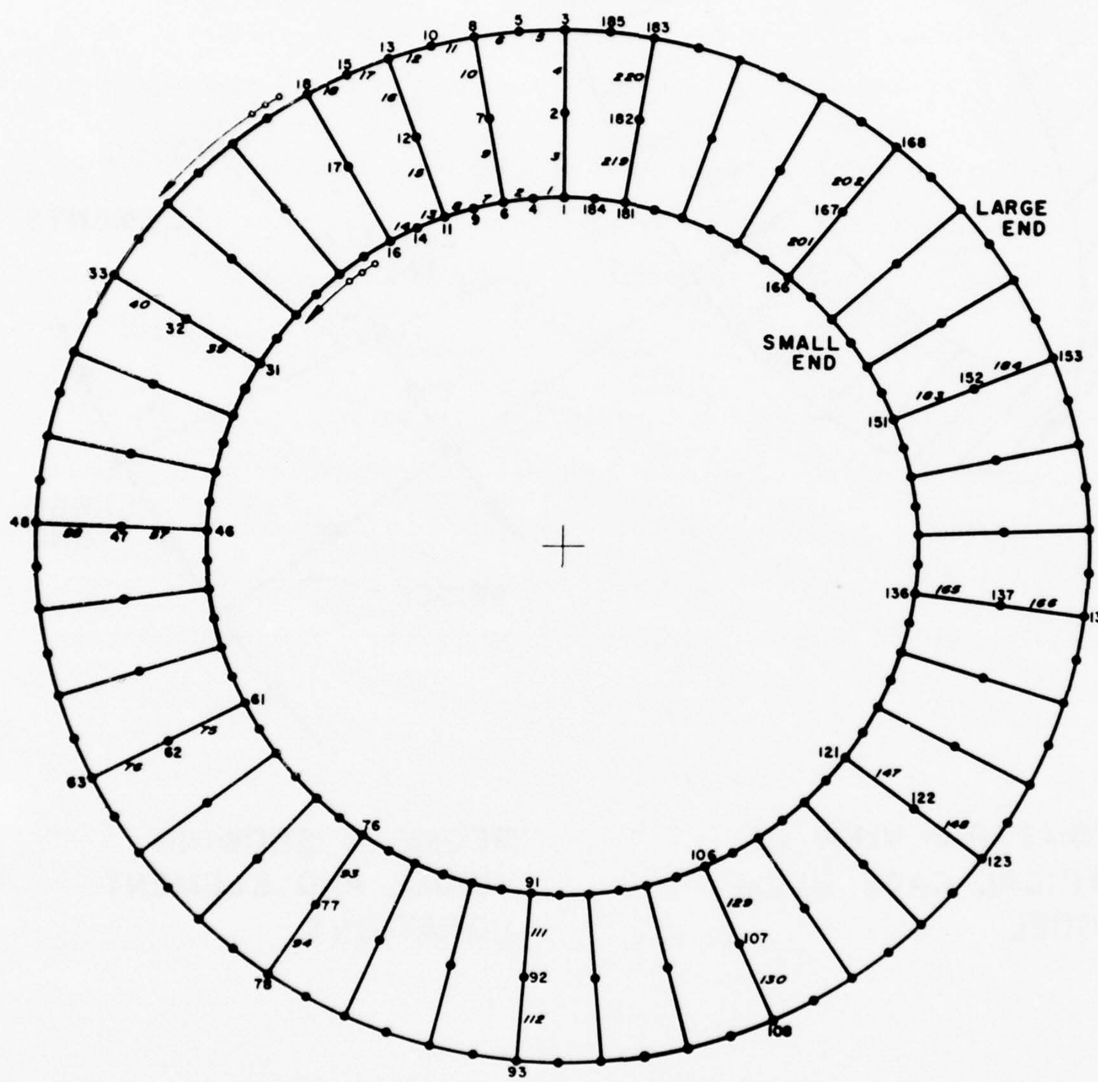

Figure 8 - Node/Element Identification for
S or L Designs (39 Rollers)

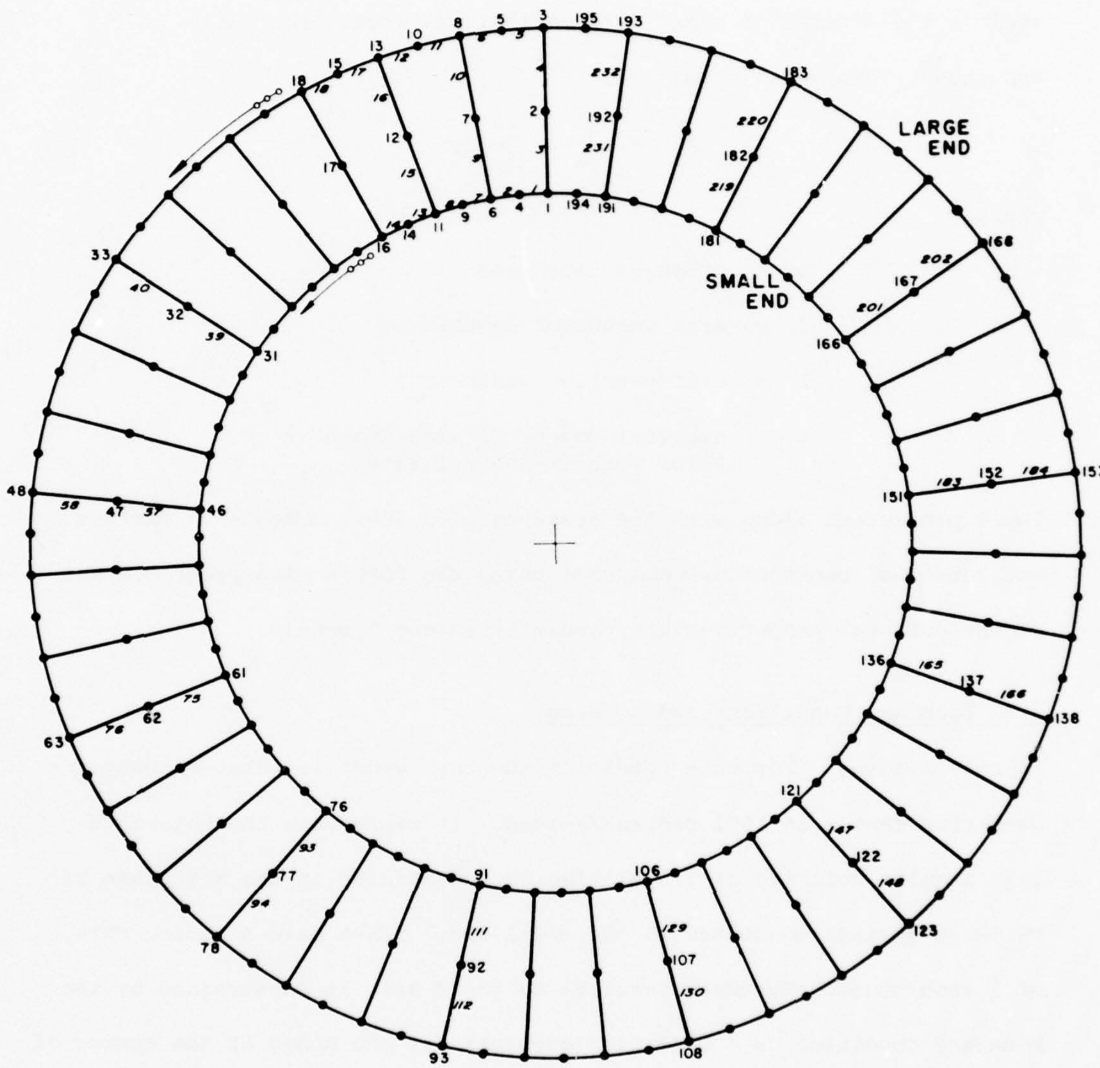

Figure 9 - Node/Element Identification
For Z Design (37 Rollers)

centroidal axis of the element and the Y and Z member axes coincide with the principal axes of the cross section. With a nonsymmetrical cross section, the location of the shear center will not coincide with the centroid. This vector distance is defined as the eccentricity. To include the effects of shear deformation, the shear area ratio is inputted. This value being

$$S_R = \frac{A}{I^2} \quad \frac{Q^2}{b} dy$$

where

A = cross-section area

I = area moment of inertia

b = cross-section width at y

Q = statical moment of area above or below y about neutral axis

These properties along with the cross-section area, moments of inertia and torsional constant are computed using the SDRC's SASA program. The cross-sectional properties are tabulated in the Appendix.

3.1 Boundary Conditions and Loading

Inertia Loading - For this condition the cage model is rotated about the geometric center at 1601 radians/second. It represents the epicyclic cage angular velocity at 3.5 million DN. Restraint in the X-Y plane is by three springs connected to the small end. These have a spring rate of 1 inch/pound. Movement parallel to the Z axis is constrained by the boundary condition UZ = 0 (Z displacement) for the nodes at the center of pockets - small end. Spring and constraint forces are in the order of magnitude of .01 lbf.

Synchronous Whirl - This case simulates synchronous forward whirl due to mass unbalance. It was applied to the models by rotating them at 1601 radians/second about a center .005" from the geometric center of the cage. This condition would be similar to an instantaneous translational acceleration in the X-Y plane of 33.2 G's. It is reached by constraining the radial displacement of a 120 degree segment diametrically opposite the unbalance force. Vectorially summing these forces

Design	Calculated Weight (lbs.)	Net Reaction (lbf.)
L	.1419	4.71
Extended L	.1652	5.48
S	.1605	5.32
Z	.2997	9.94

Material - Steel (.283 lbs./in.^{3})

Axial displacement is constrained as in the previous load condition.

The eccentricity of .005" was used to represent the radial clearance in a roller guided cage or the maximum pilot-guide clearance in a race guided cage.

3.2 Stresses and Deformation

Figure 10 illustrates a typical distorted geometry plot (L-cage, eccentric rotation). In the displacement solutions a slight amount of translation and rotation of the nodes/elements occurs. Therefore in order to obtain the actual cage deformation the translated center is computed from the undistorted geometry and the displacement solution. The maximum displacement at the large-end bridge conjunction is shown in the following results. The beam analysis results are given on Table 1.

The F_x/A column represents the mean stress over the entire cross-sectional area. Max. and Min. S_x indicates the effects of bending. The beam elements are subdivided into four quadrants and the tensile (+) or compressive(-) stresses computed. Normal mean stresses in the Y and Z directions along with shear effects have been excluded from these summaries as they add little to the results.

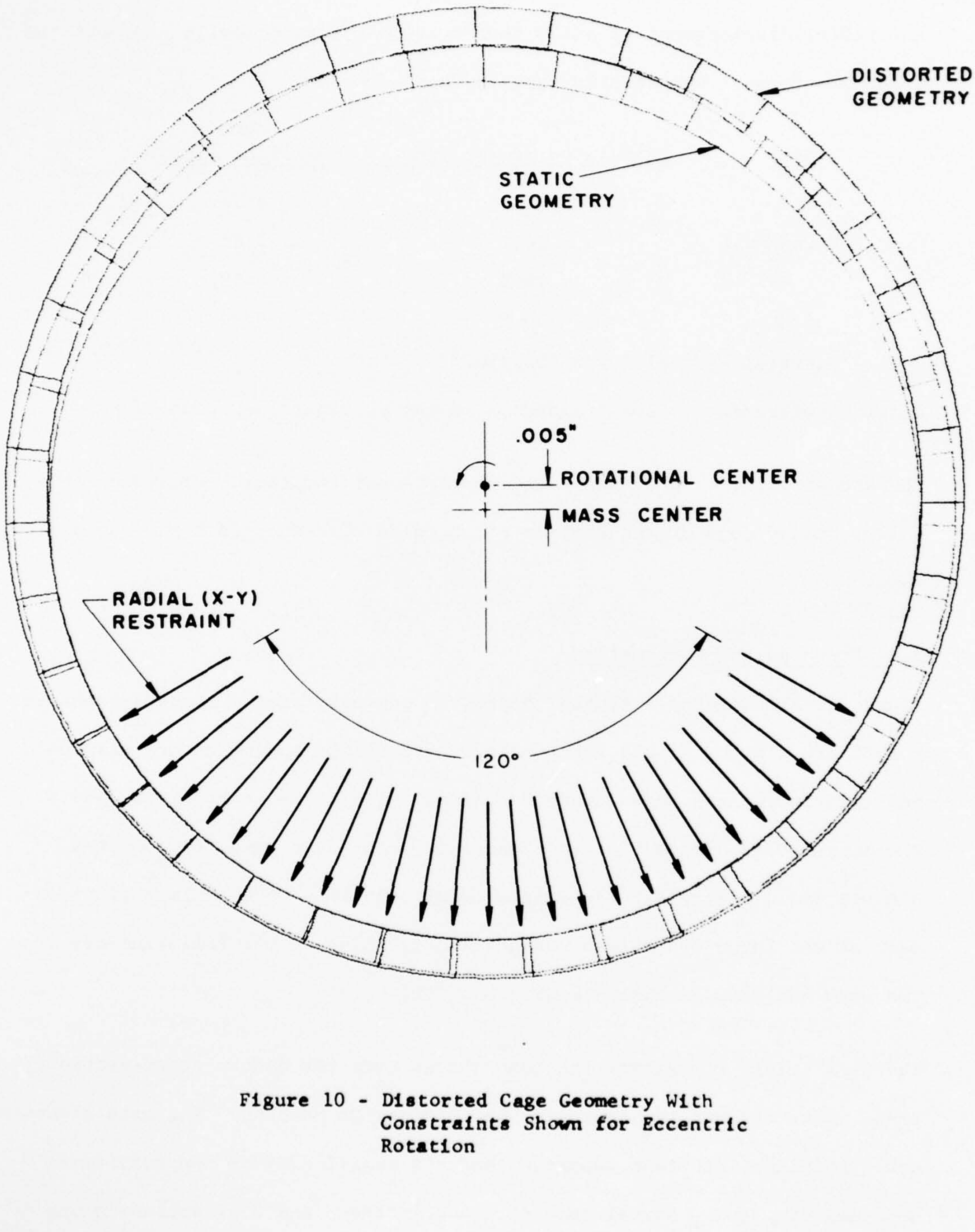

Figure 10 - Distorted Cage Geometry With Constraints Shown for Eccentric Rotation

TABLE 1

Stress and Deformation Results
for Beam Elements

Units - Stresses (PSI), Deformation (In.)

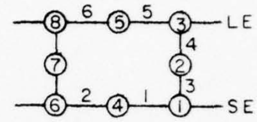

Element	Node	F_x/A	Max. S_x	Min. S_x	Radial Deformation
	Design:	L, Steel			
	Loading:	Inertial, 1601 Radians/Second			
1	1	20,330	28,565	12,095	
1	4	20,330	29,544	11,116	
3	1	485	2,208	- 1,238	
3	2	7	30,276	-30,261	
4	2	7	30,276	-30,261	
4	3	-485	507	- 1,485	
5	3	26,237	33,444	19,031	.0023
5	5	26,237	37,371	15,104	
	Design:	S, Steel			
	Loading:	Inertial, 1601 Radians/Second			
1	1	20,301	27,970	12,631	
1	4	20,301	28,933	11,669	
3	1	496	2,094	- 1,106	
3	2	5	30,112	-30,102	
4	2	5	30,112	-30,102	
4	3	-508	1,125	- 2,141	
5	3	21,879	29,536	14,222	.0020
5	5	21,879	28,770	14,988	
	Design:	Z, Steel			
	Loading:	Inertial, 1601 Radians/Second			
1	1	16,360	23,307	9,412	
1	4	16,360	22,494	10,226	
*3	1	346	5,190	- 4,497	
*3	2	9	23,530	-23,513	
4	2	9	23,530	-23,513	
4	3	-338	2,233	- 2,910	
5	3	19,334	24,158	14,509	.0017
5	5	19,334	27,458	11,209	

* Stresses will be slightly greater if the slot is machined in O.D. to unitize the cone - cage - roller assembly

TABLE 1 (Con't.)

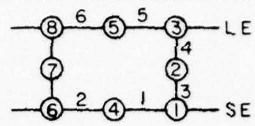

Element	Node	F_x/A	Max. S_x	Min. S_x	Radial Deformation
	Design:	L-Extended*, Steel			
	Loading:	Inertial, 1601 Radians/Second			
1	1	20,502	28,809	12,196	
1	4	20,502	29,803	11,202	
3	1	493	2,231	- 1,245	
3	2	- 4	31,489	-31,496	
4	2	- 4	31,489	-31,496	
4	3	-521	3,609	- 4,651	
5	3	22,165	30,742	13,589	.0023
5	5	22,165	33,856	10,475	
	Design:	L, Steel			
	Loading:	Synchronous Whirl, 1601 Radians/ Second at .005" Eccentricity			
1	1	20,270	28,889	11,650	
1	4	20,270	29,903	10,636	
3	1	481	2,086	- 1,124	
3	2	2	30,319	-30,315	
4	2	2	30,319	-30,315	
4	3	-495	636	- 1,626	
5	3	26,330	34,088	18,571	.0061
5	5	26,330	36,930	15,730	
	Design:	L-Extended*, Steel			
	Loading:	Synchronous Whirl, 1601 Radians/ Second at .005" Eccentricity			
1	1	20,433	29,151	11,715	
1	4	20,433	30,184	10,683	
3	1	488	2,095	- 1,118	
3	2	- 9	31,535	-31,553	
4	2	- 9	31,535	-31,553	
4	3	-528	3,757	- 4,811	
5	3	22,233	31,396	13,070	.0057
5	5	22,233	33,354	11,112	

* The L-Extended design is similar to the L design except for an extension of the LE flange width by .0625"

TABLE 1 (Con't.)

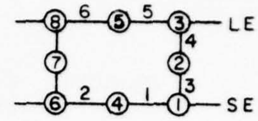

Element	Node	F_x/A	Max. S_x	Min. S_x	Radial Deformation
	Design:	L, Steel			
	Loading:	Synchronous Whirl, 1373 Radians/ Second at .005" Eccentricity			
1	1	14,907	21,247	8,568	
1	4	14,907	21,992	7,823	
3	1	354	1,534	- 827	
3	2	2	22,299	-22,295	
4	2	2	22,299	-22,295	
4	3	-364	468	- 1,196	
5	3	19,364	25,070	13,658	
5	5	19,364	27,160	11,568	
	Design:	L, Aluminum (.094 lbs./in.^{3})			
	Loading:	Synchronous Whirl, 1601 Radians/ Second at .005" Eccentricity			
1	1	6,747	9,615	3,880	
1	4	6,747	9,951	3,544	
3	1	160	695	- 375	
3	2	1	10,093	-10,091	
4	2	1	10,093	-10,091	
4	3	-165	211	- 540	
5	3	8,764	11,345	6,183	
5	5	8,764	12,295	5,234	.0061
	Design:	S, Steel			
	Loading:	Synchronous Whirl, 1601 Radians/ Second at .005" Eccentricity			
1	1	20,254	28,243	12,264	
1	4	20,254	29,242	11,265	
3	1	493	1,979	- 994	
3	2	0	30,188	-30,188	
4	2	0	30,188	-30,188	
4	3	-513	1,191	- 2,218	
5	3	21,924	29,251	14,597	.0056
5	5	21,924	27,519	16,329	

TABLE 1 (Con't.)

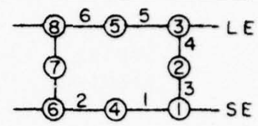

Design: Z, Steel
Loading: Synchronous Whirl, 1601 Radians/ Second at .005" Eccentricity

Element	Node	F_x/A	Max. S_x	Min. S_x	Radial Deformation
1	1	16,316	23,194	9,437	
1	4	16,316	22,387	10,245	
*3	1	339	4,780	- 4,102	
*3	2	1	23,669	-23,667	
4	2	1	23,669	-23,667	
4	3	-347	2,440	- 3,134	
5	3	19,394	25,166	13,622	.0046
5	5	19,394	27,202	11,586	

* Stresses will be slightly greater if the slot is machined in O.D. to unitize the cone - cage - roller assembly

SECTION IV

SOLID MODELS

Having symmetric geometry and boundary conditions permitted the analysis to be performed on a segment of the cage designs. The three bridge segment was chosen to eliminate end effects on the central bridge. Geometry plots of the designs investigated are shown in Figures 11, 12 and 13. The origin of the absolute Cartesian coordinate system is shown on each plot. It is coincident with the cage center, the X-Y plane intersects the small end and the X-Z plane intersects the left-hand side. All stresses and strains computed are in these coordinate systems.

A solid with a parabolic displacement order was used as the modeling element. The element/node conventions are shown in Figure 14.

4.1 Boundary Conditions and Loading

At each end of the segments modeled three constraints are applied. In the rotated nodal coordinate systems these are Y translation and X and Z rotations equal zero. This is graphically illustrated in Figure 15.

Two loading conditions were imposed on the solid element models. These have been identified as inertial and normal bridge loading.

The inertial condition is similar to that as applied to the beam element. The model is rotated about the absolute Z axis at 1601 radians/second.

The bridge loading case consisted of applying a five pound force normal to the roller-bridge conjunction. To maximize its effect the load was applied as a concentrated force at the center of the bridge. In nodal coordinates this is a 1.65 lbf. Y component and a 4.72 lbf. X component for the roller guided design. The race guided design was subjected to a 5 lb. Y direction

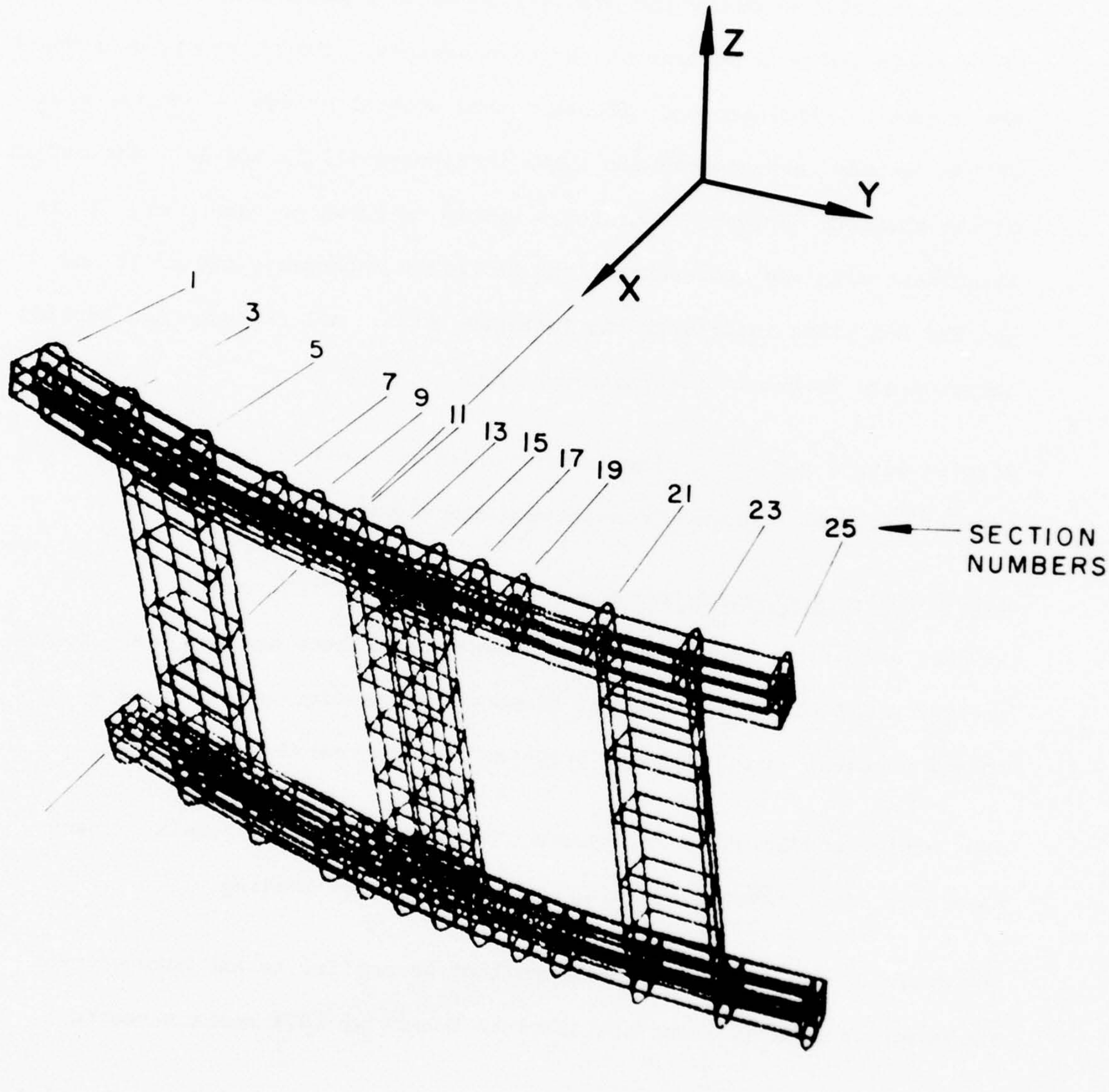

Figure 11 - L-Cage Geometry Plot

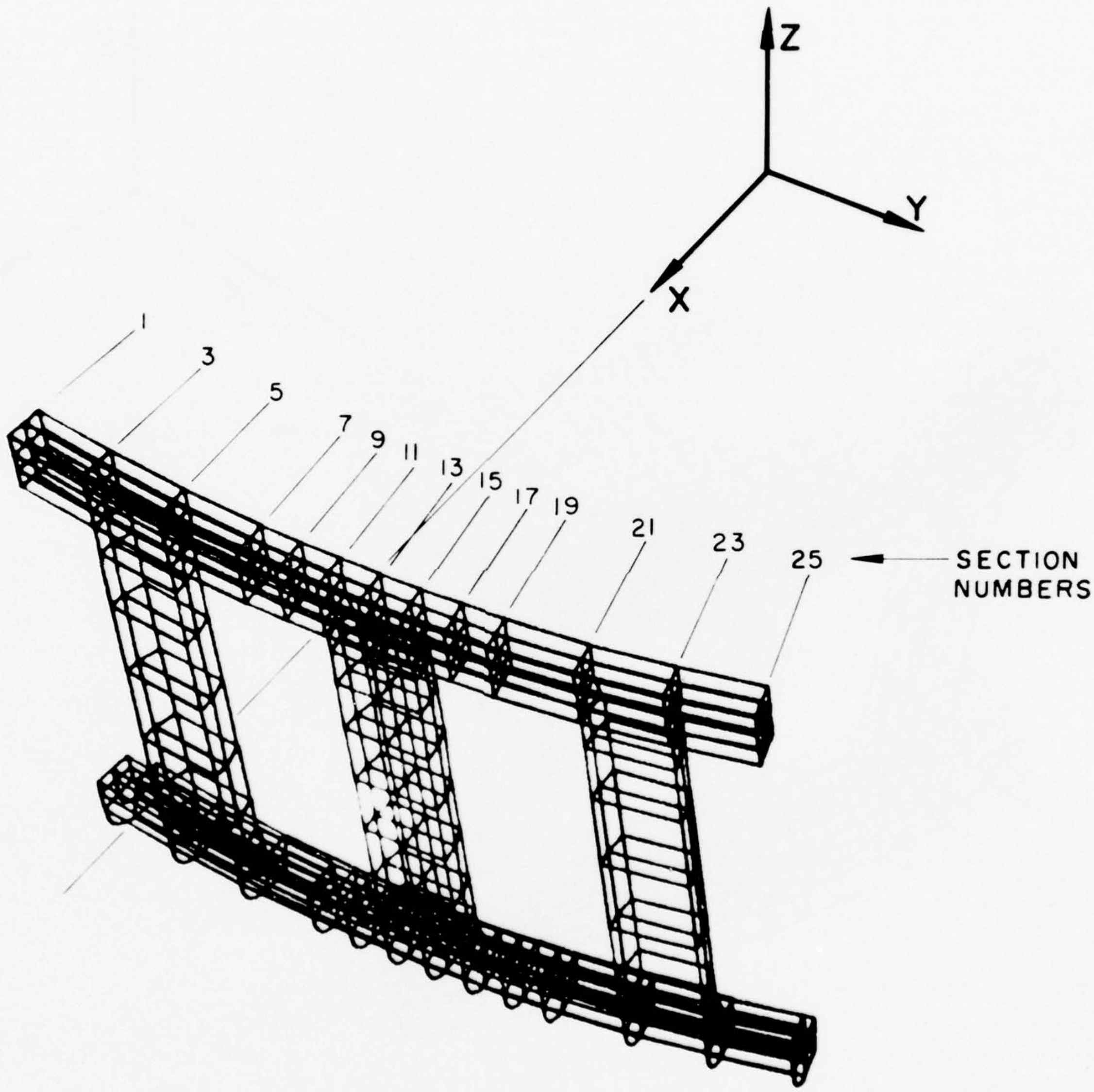

Figure 12 - S-Cage Geometry Plot

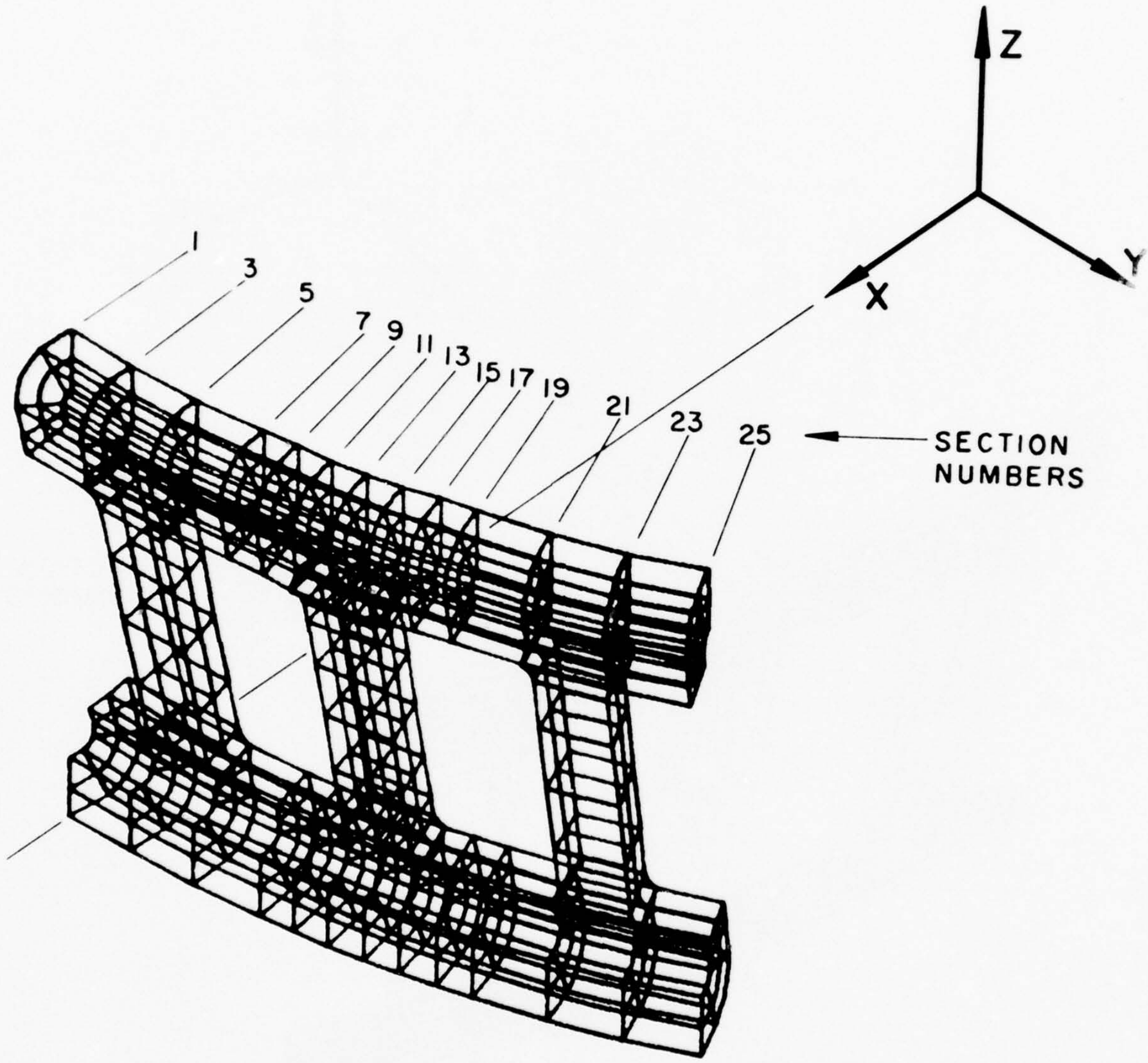

Figure 13 - Z-Cage Geometry Plot

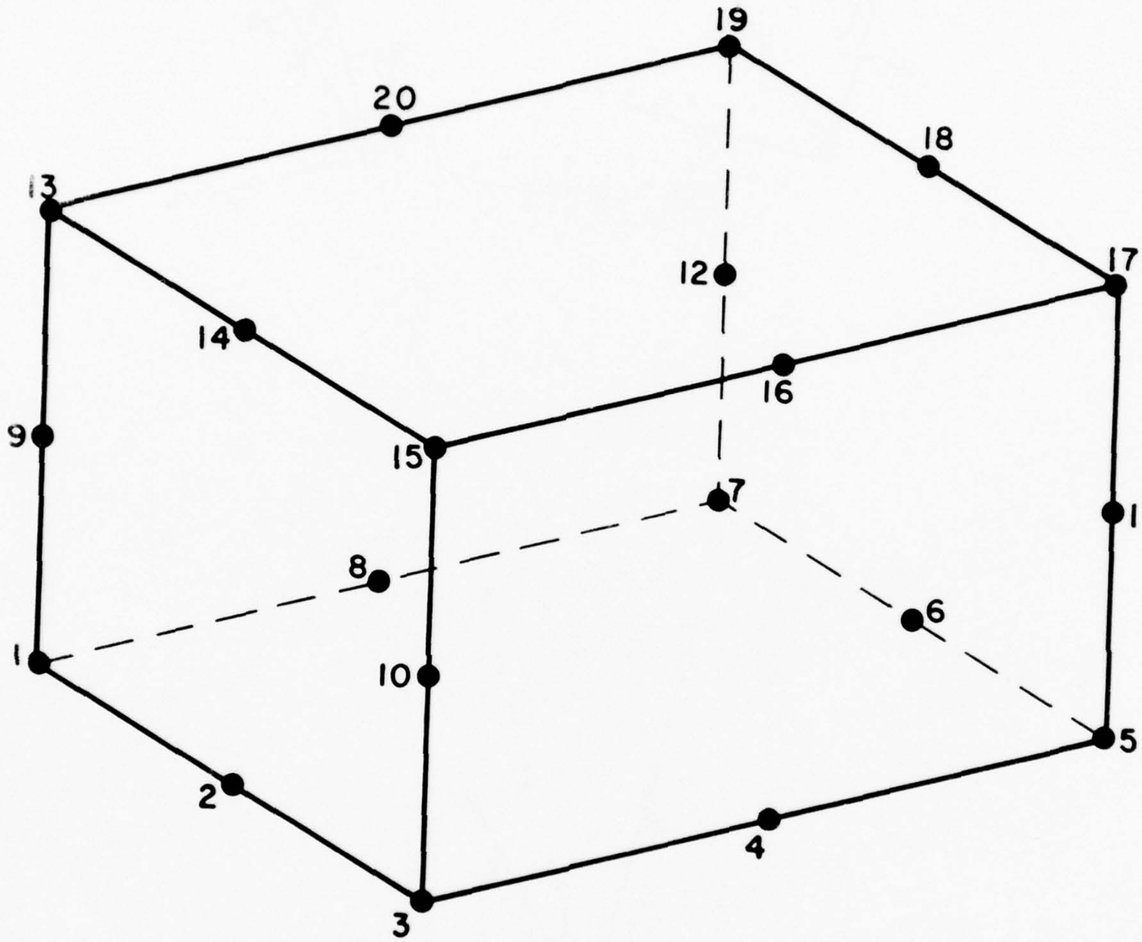

Figure 14 - Typical Solid Element
With Nodes Identified

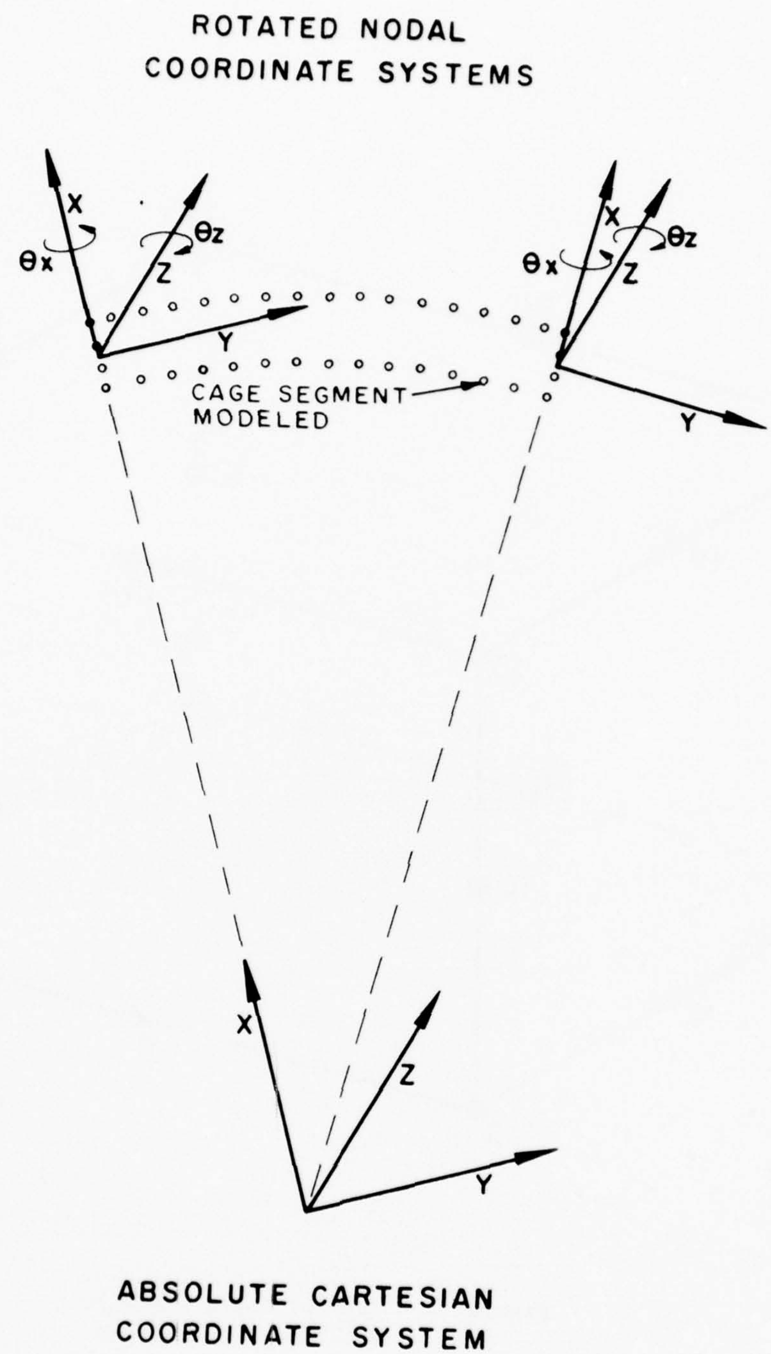

Figure 15 - Coordinate Systems and Solid Element Model Constraints

force. The decision to use a 5 lb. force was based on two prior investigations. In reference 10 an instrumented 100 millimeter bearing was tested at speeds to 20,000 RPM and forces of approximately 5 lbs. were measured. Random impact loads as high as 50 lbs. were observed. In a Timken Company investigation conducted according to a modified version of ASTM D 2782-74, test blocks made of SAE 1020 steel and silver plated were subjected to an equivalent normal roller load of 2 lbf. (14,000 psi). The plating could not sustain the rotating test cup. In post test cage inspections, seldom is the silver plating removed. This would be indicative of light bridge-roller interactions.

4.2 Stresses and Deformation

Output from the SDRC SUPERB program consists of nodal displacements and rotations in the local coordinate system. The normal, shear, principal and Von Mises stresses are in the absolute system. The L cage was modeled with 226 elements (1735 nodes); the S and Z cages with 250 elements (1743 nodes). Computed displacements and stresses for the three designs under two loading conditions produced a vast amount of data. This data has been condensed into 14 stress plots and two summary tables per design. The compiled data is from segment sections 7 through 19. The primary stresses are tensile hoop stresses in both the large and small end flanges and bending in the bridge.

Distorted geometry for the three designs are shown in Figure 16. Stress plots are as follows: Figures 16-30, L-cage; Figures 31-44, S-cage; and Figures 45-58, Z-cage.

Maximum displacement (U_x), principal stress (σ_1 or σ_2) and Von Mises stress for segments 7 to 19 are given on Tables 2 through 6.

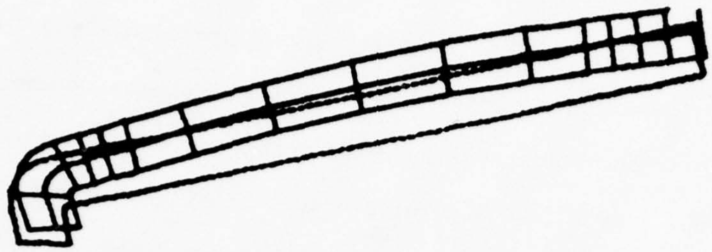

L-CAGE

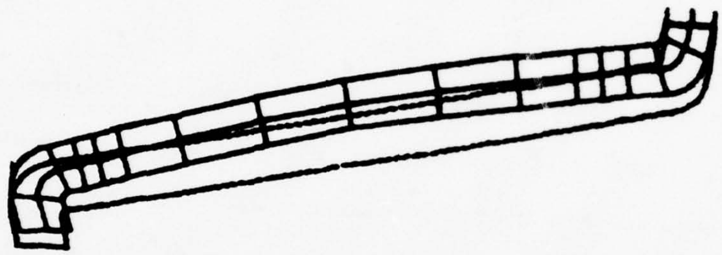

S-CAGE

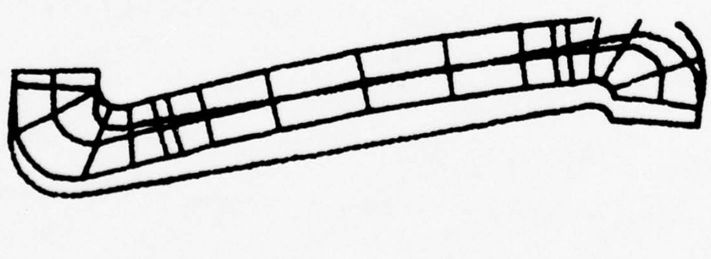

Z-CAGE

Figure 16 - Distorted Geometry Inertial Loading

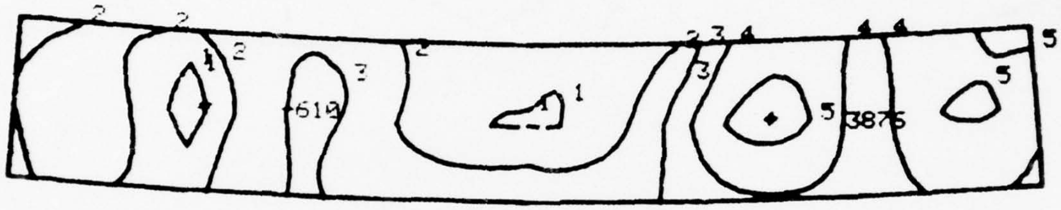

Sec. 7 O.D. Sec. 19

CONTOUR INTERVAL = 880 (psi)

CONTOUR NUMBER	CONTOUR LEVEL
1	0.00000000
2	880
3	1769
4	2640
5	3520

Figure 17 - L-Cage, X-Normal Stress, Inertial Loading, Large End Adjacent Bridge

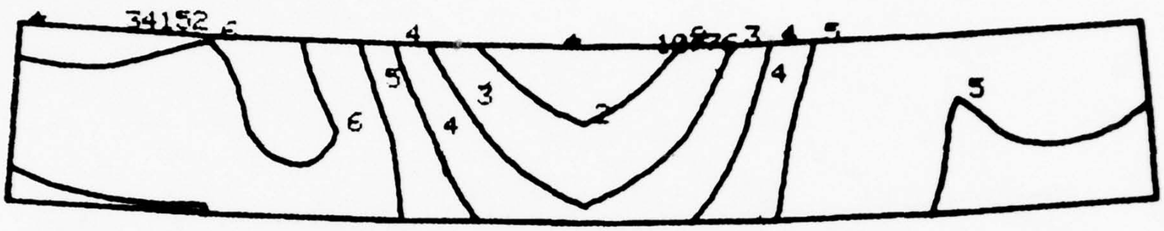

Sec. 7 O.D. Sec. 19

CONTOUR INTERVAL = 4600 (psi)

CONTOUR NUMBER	CONTOUR LEVEL
1	9200
2	13800
3	18400
4	23000
5	27600
6	32200

Figure 18 - L-Cage, Y-Normal Stress, Inertial Loading, Large End Adjacent Bridge

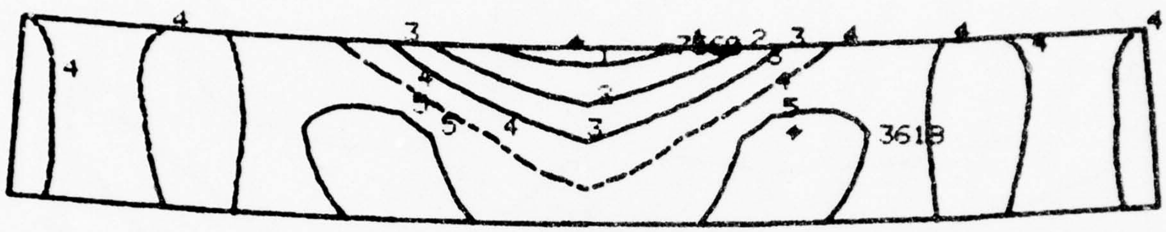

Sec. 7 O.D. Sec. 19

CONTOUR INTERVAL = 2200 (psi)

CONTOUR NUMBER	CONTOUR LEVEL
1	-6600
2	-4400
3	-2200
4	0.00000000
5	2200

Figure 19 - L-Cage, Z-Normal Stress Inertial Loading, Large End Adjacent Bridge

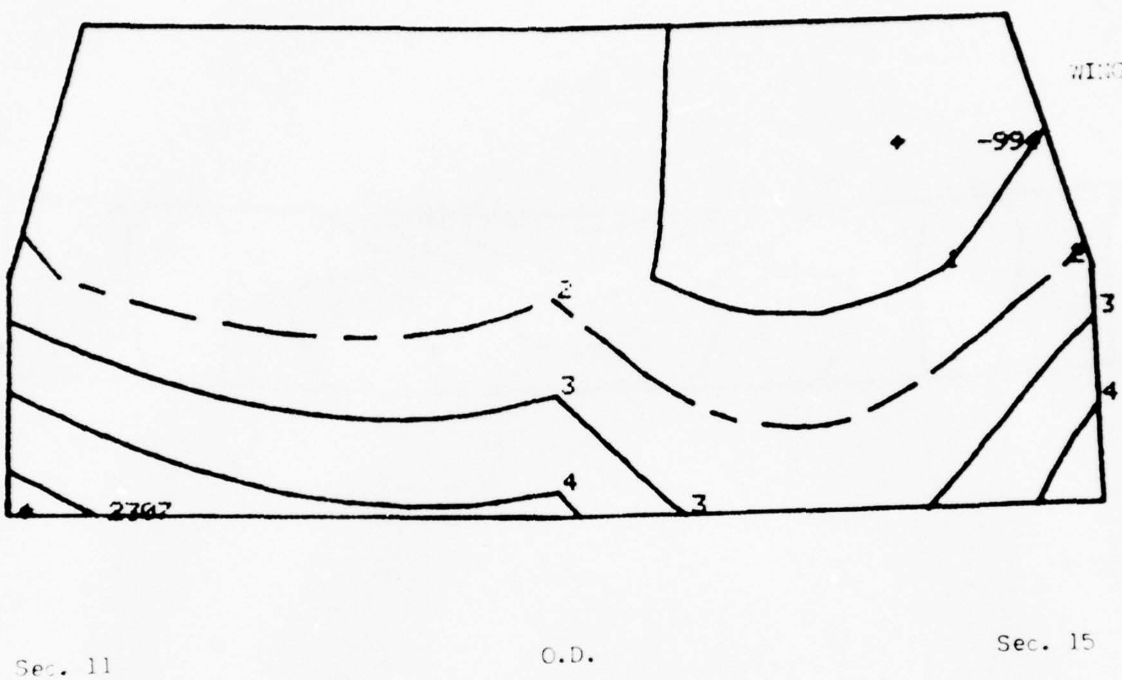

CONTOUR INTERVAL = 660 (psi)

CONTOUR NUMBER	CONTOUR LEVEL
1	-660
2	0.00000000
3	660
4	1320
5	1980

Figure 20 - L-Cage, X-Normal Stress Inertial Loading, Bridge Adjacent Large End

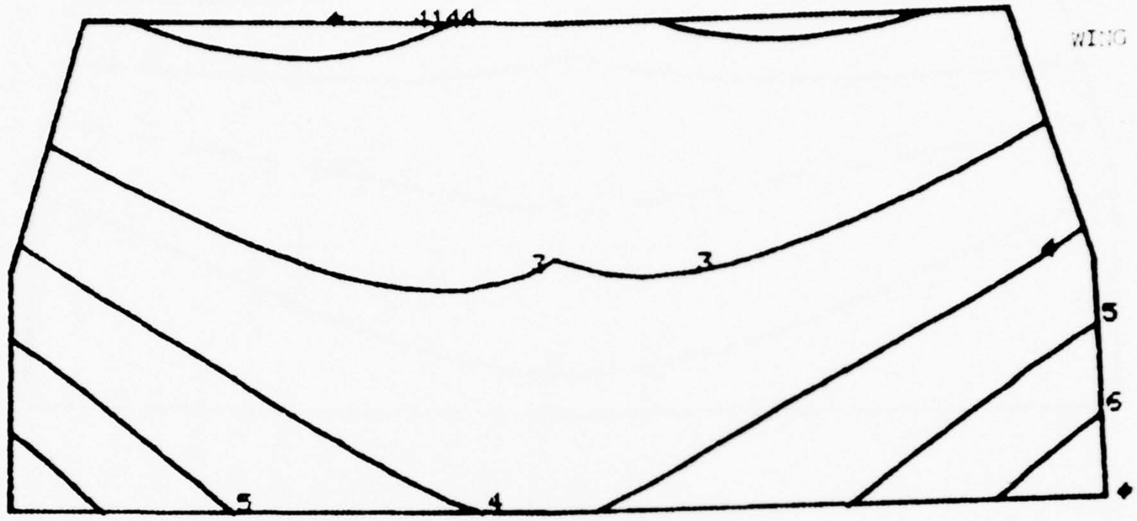

Sec. 11 O.D. Sec. 15

CONTOUR INTERVAL = 4800 (psi)

CONTOUR NUMBER	CONTOUR LEVEL
1	0.00000000
2	4800
3	9600
4	14400
5	19200
6	24000

Figure 21 - L-Cage, Y-Normal Stress Inertial Loading, Bridge Adjacent Large End

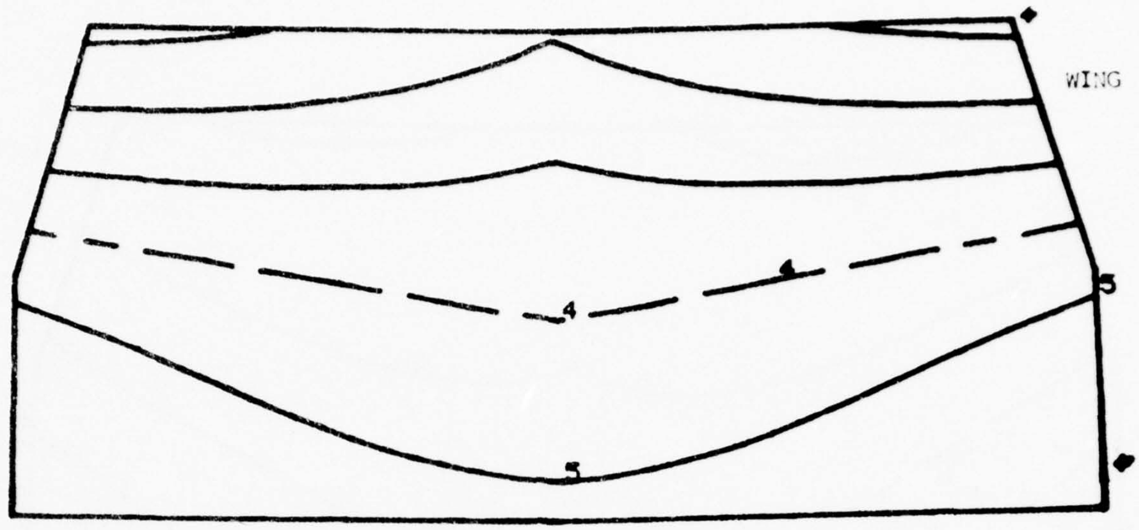

Sec. 11 O.D. Sec. 15

CONTOUR INTERVAL = 3100 (psi)

CONTOUR NUMBER	CONTOUR LEVEL
1	-9300
2	-6200
3	-3100
4	0.00000000
5	3100

Figure 22 - L-Cage, Z-Normal Stress Inertial Loading, Bridge Adjacent Large End

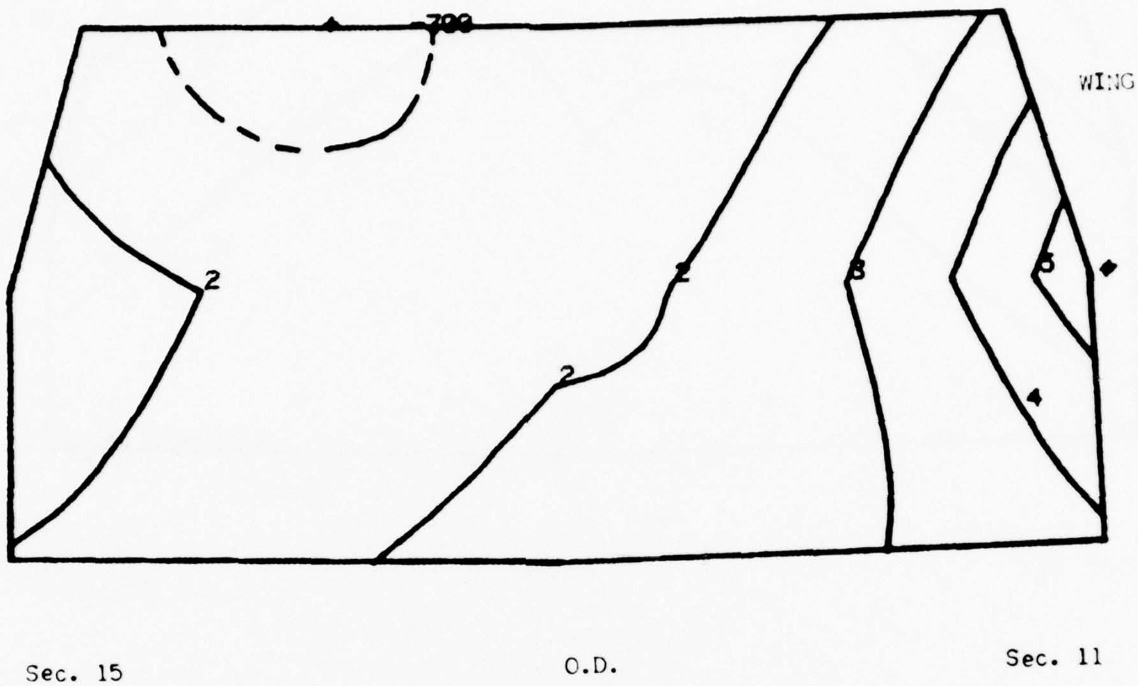

CONTOUR INTERVAL = 840 (psi)

CONTOUR NUMBER	CONTOUR LEVEL
1	0.00000000
2	840
3	1680
4	2520
5	3360

Figure 23 - L-Cage, X-Normal Stress, Inertial Loading, Bridge Adjacent Small End

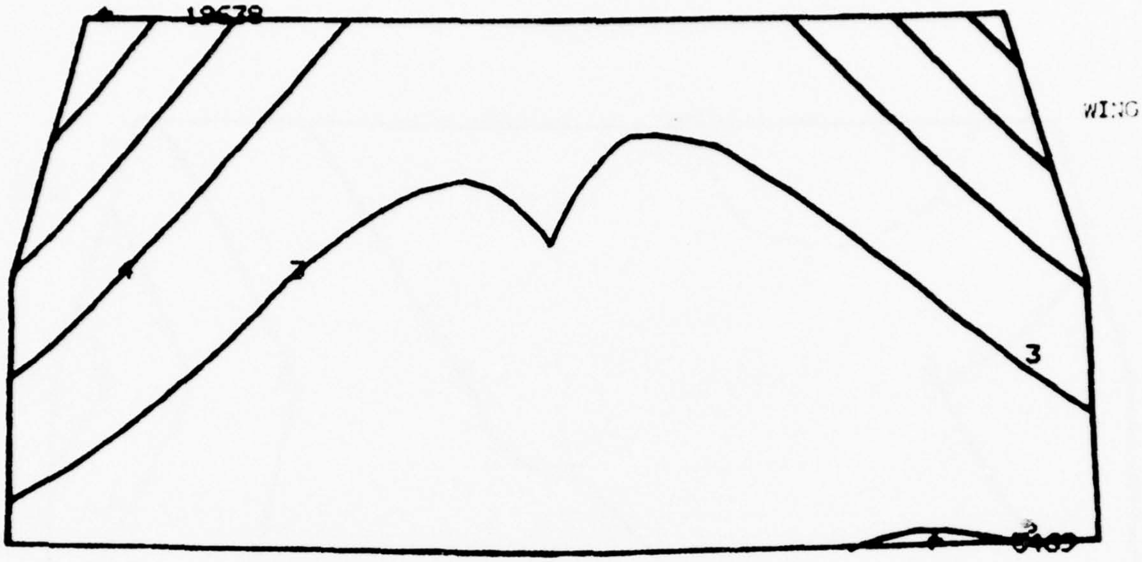

Sec. 15 O.D. Sec. 11

CONTOUR INTERVAL = 2800 (psi)

CONTOUR NUMBER	CONTOUR LEVEL
1	2800
2	5600
3	8400
4	11200
5	14000
6	16800
7	19600

Figure 24 - L-Cage, Y-Normal Stress Inertial Loading, Bridge Adjacent Small End

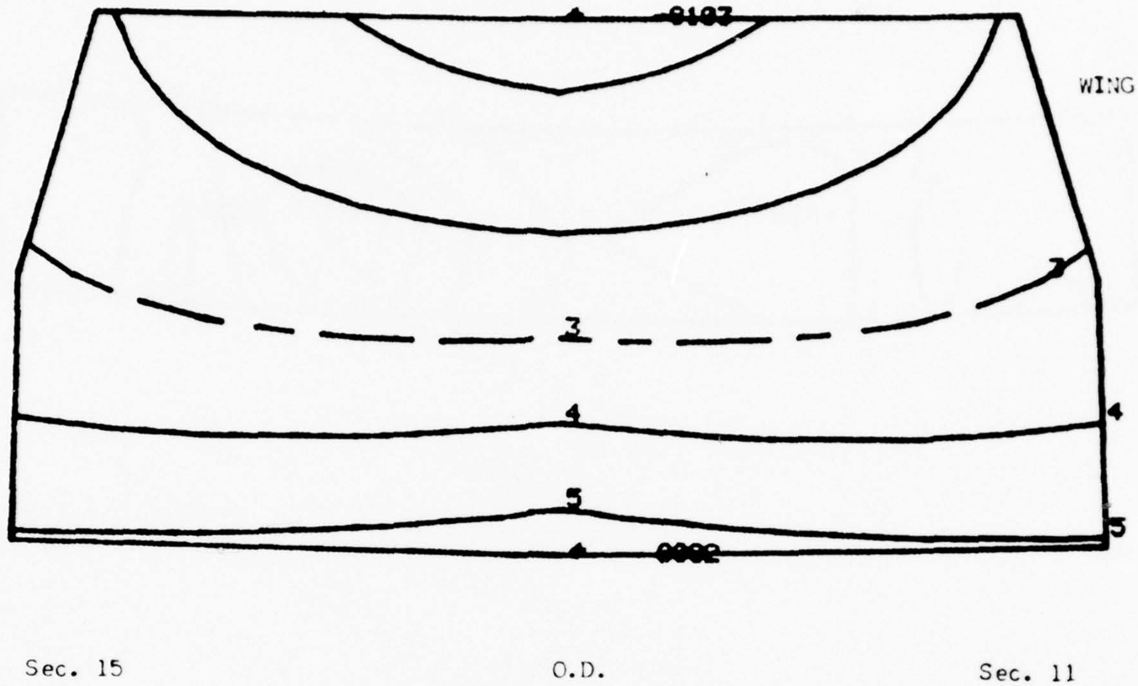

CONTOUR INTERVAL = 3200 (psi)

CONTOUR NUMBER	CONTOUR LEVEL
1	-6400
2	-3200
3	0.00000000
4	3200
5	6400

Figure 25 - L-Cage, Z-Normal Stress, Inertial Loading, Bridge Adjacent Small End

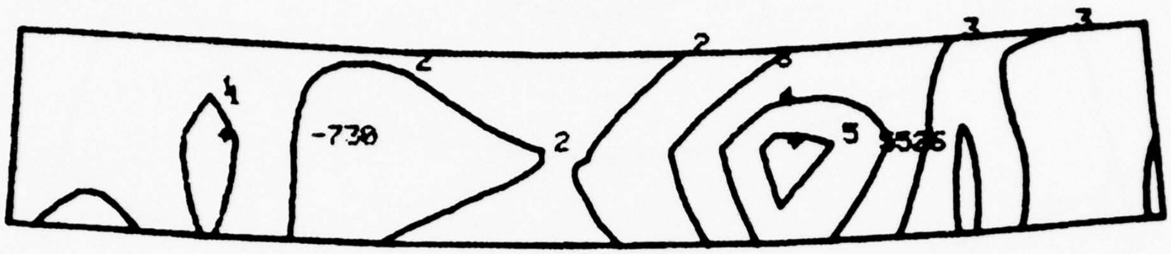

Sec. 7 O.D. Sec. 19

CONTOUR INTERVAL = 1250 (psi)

CONTOUR NUMBER	CONTOUR LEVEL
1	0.00000000
2	1250
3	2500
4	3750
5	5000

Figure 26 - L-Cage, X-Normal Stress Inertial Loading, Small End Adjacent Bridge

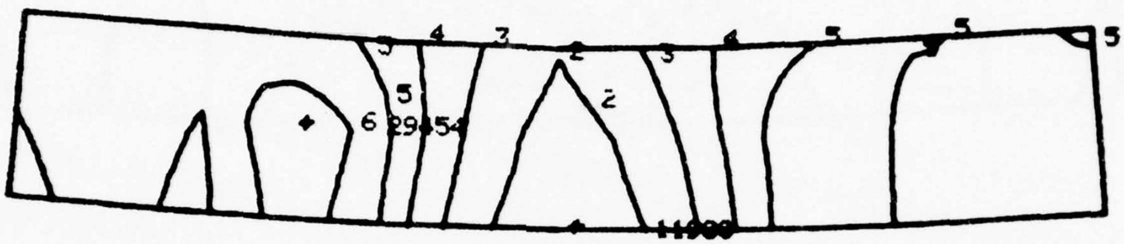

Sec. 7 O.D. Sec. 19

CONTOUR INTERVAL = 3500 (psi)

CONTOUR NUMBER	CONTOUR LEVEL
1	10500
2	14000
3	17500
4	21000
5	24500
6	28000

Figure 27 - L-Cage, Y-Normal Stress, Inertial Loading, Small End Adjacent Bridge

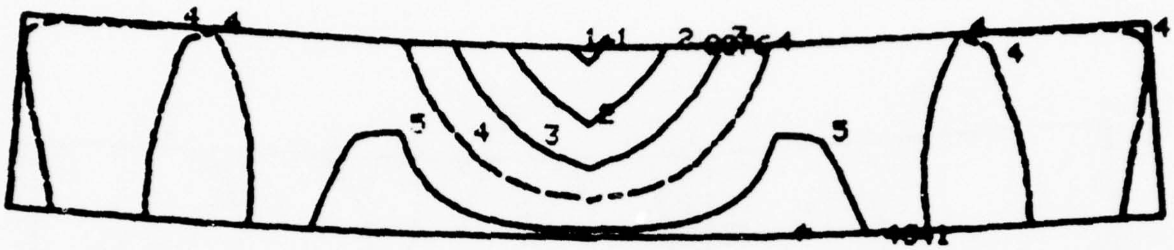

Sec. 7 O.D. Sec. 19

CONTOUR INTERVAL = 2500 (psi)

CONTOUR NUMBER	CONTOUR LEVEL
1	-7500
2	-5000
3	-2500
4	0.00000000
5	2500

Figure 28 - L-Cage, Z-Normal Stress, Inertial Loading, Small End Adjacent

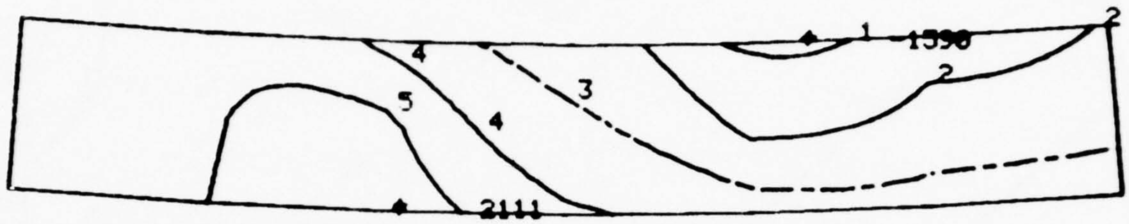

Sec. 7 O.D. Sec. 19

CONTOUR INTERVAL = 740 (psi)

CONTOUR NUMBER	CONTOUR LEVEL
1	-1480
2	-740
3	0.00000000
4	740
5	1480

Figure 29 - L-Cage, Y-Normal Stress Bridge Loading, Large End Adjacent Bridge

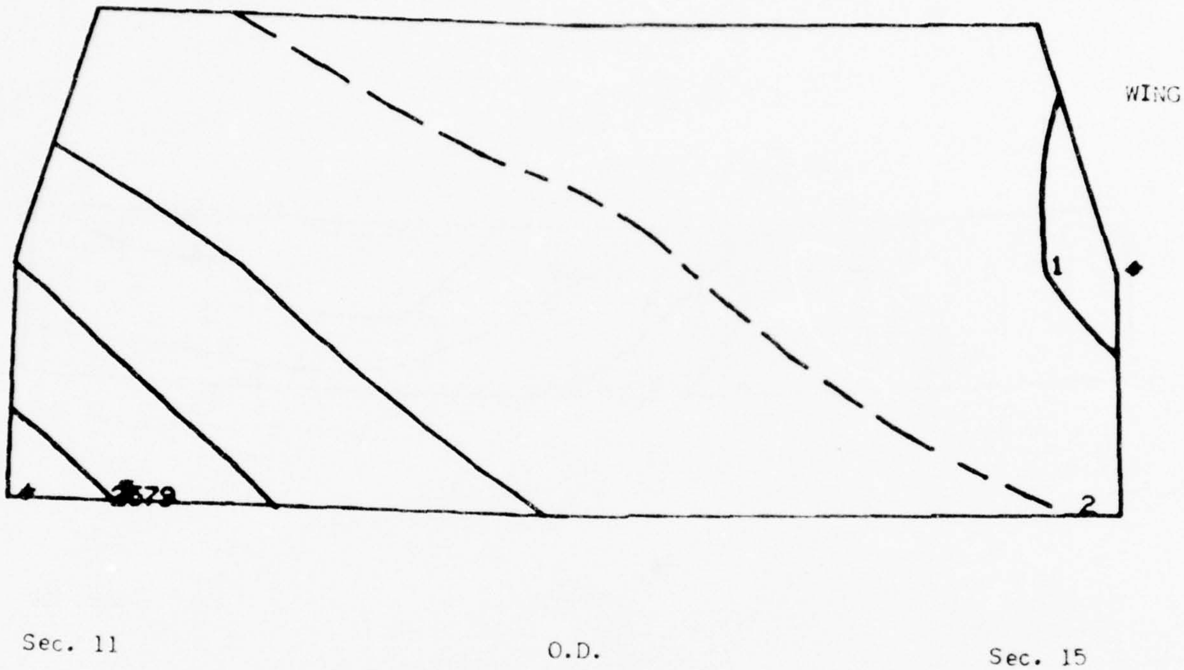

CONTOUR INTERVAL = 680 (psi)

CONTOUR NUMBER	CONTOUR LEVEL
1	-680
2	0.00000000
3	680
4	1360
5	2040

Figure 30 - L-Cage, Y-Normal Stress, Bridge Loading, Bridge Adjacent Large End

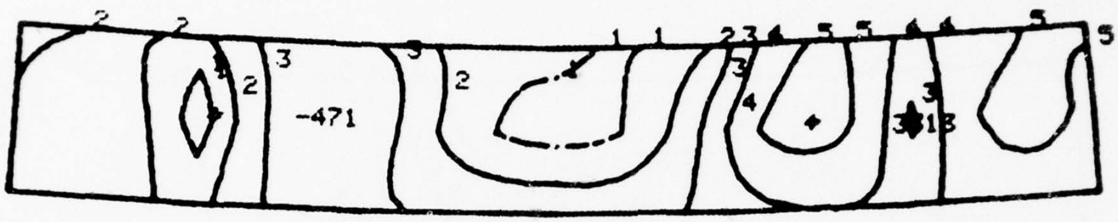

Sec. 7 O.D. Sec. 19

CONTOUR INTERVAL = 740 (psi)

CONTOUR NUMBER	CONTOUR LEVEL
1	0.00000000
2	740
3	1480
4	2220
5	2960

Figure 31 - S-Cage, X-Normal Stress, Inertial Loading, Large End Adjacent Bridge

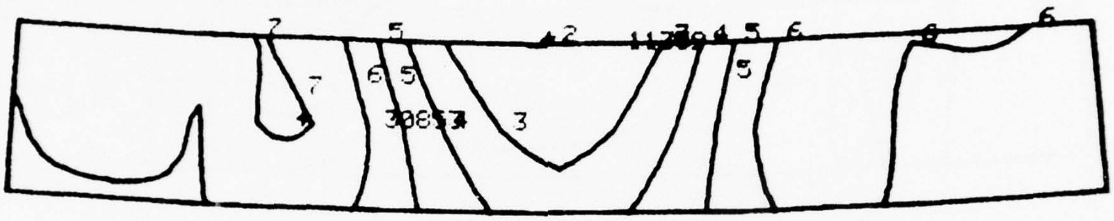

Sec. 7 O.D. Sec. 19

CONTOUR INTERVAL = 3800 (psi)

CONTOUR NUMBER	CONTOUR LEVEL
1	7600
2	11400
3	15200
4	19000
5	22800
6	26600
7	30400

Figure 32 - S-Cage, Y-Normal Stress Inertial Loading, Large End Adjacent Bridge

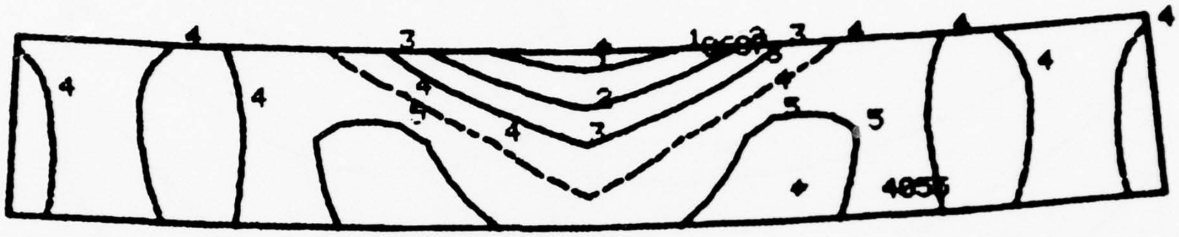

Sec. 7 O.D. Sec. 19

CONTOUR INTERVAL = 2500 (psi)

CONTOUR NUMBER	CONTOUR LEVEL
1	-7500
2	-5000
3	-2500
4	0.00000000
5	2500

Figure 33 - S-Cage, Z-Normal Stress, Inertial Loading, Large End Adjacent Bridge

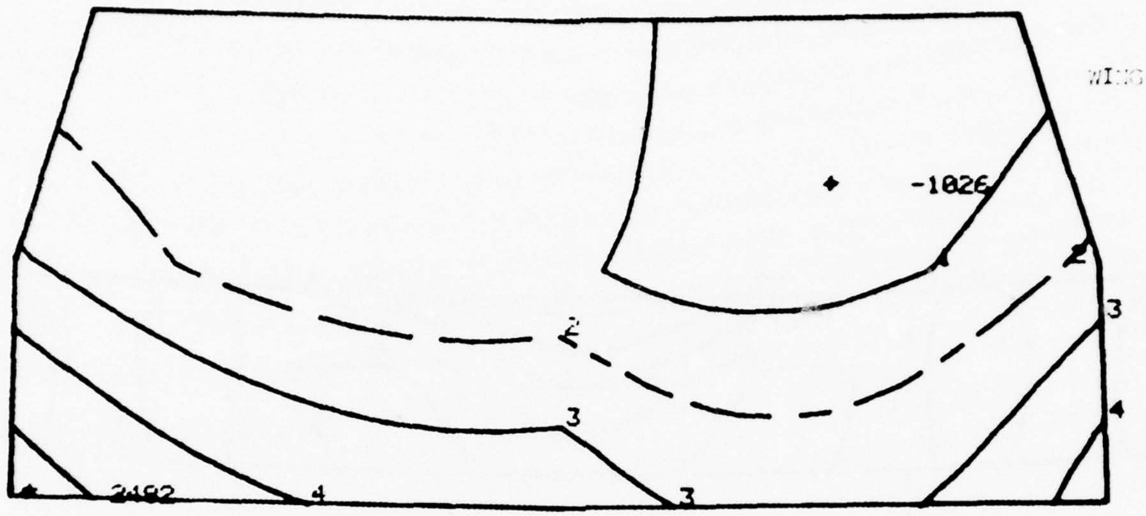

Sec. 11 O.D. Sec. 15

CONTOUR INTERVAL = 700 (psi)

CONTOUR NUMBER	CONTOUR LEVEL
1	-700
2	0.00000000
3	700
4	1400
5	2100

Figure 34 - S-Cage, X-Normal Stress, Inertial Loading, Bridge Adjacent Large End

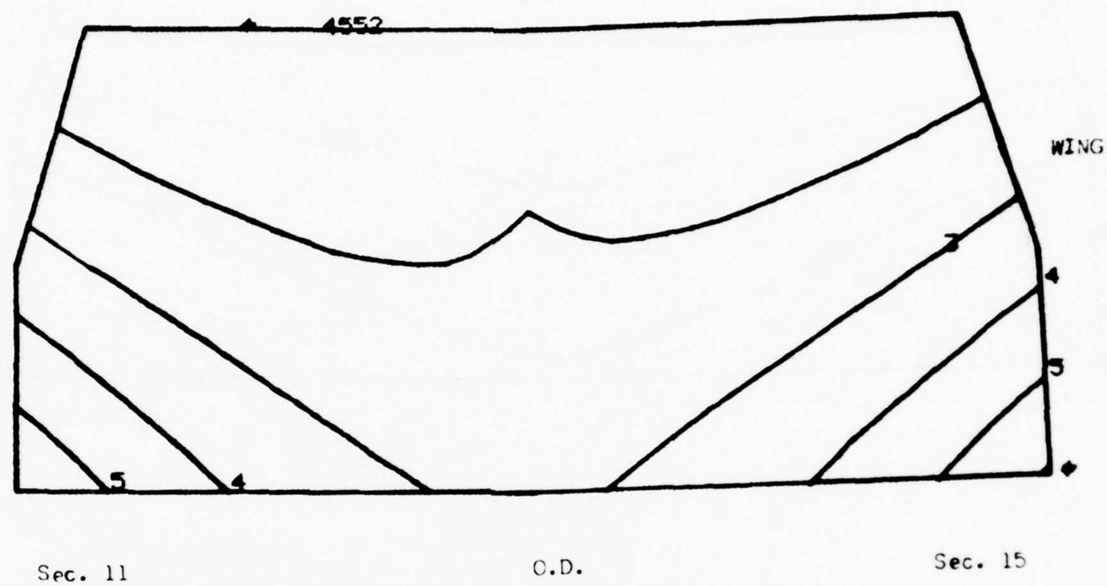

CONTOUR INTERVAL = 4400 (psi)

CONTOUR NUMBER	CONTOUR LEVEL
1	4400
2	8800
3	13200
4	17600
5	22000
6	26400

Figure 35 - S-Cage, Y-Normal Stress, Inertial Loading, Bridge Adjacent Large End

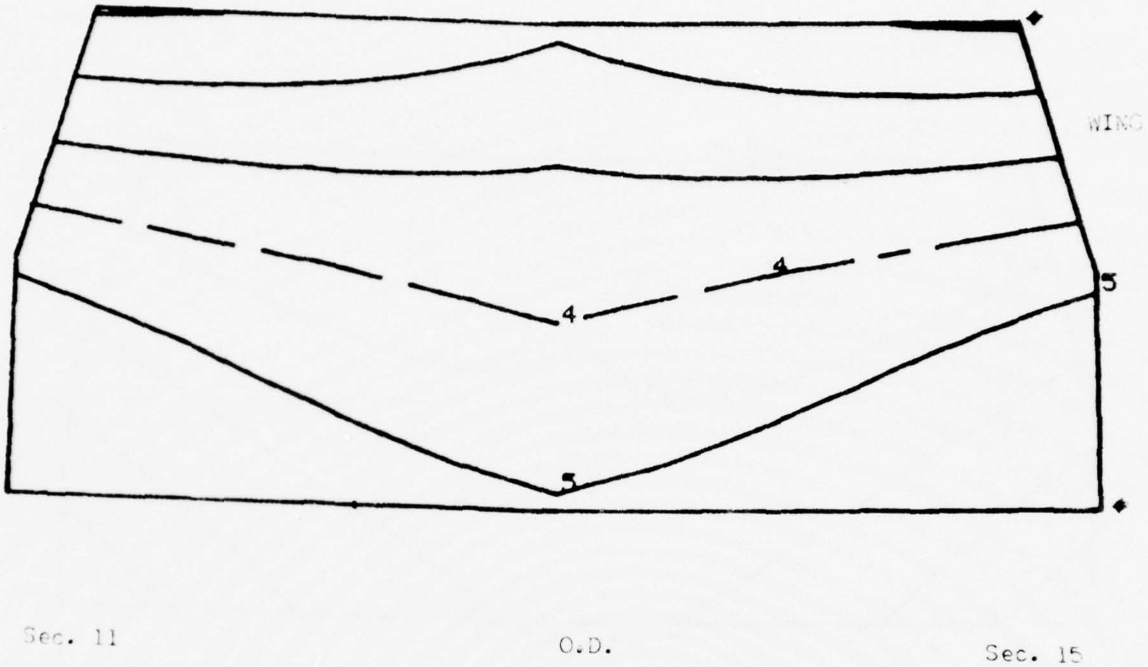

CONTOUR INTERVAL = 3500 (psi)

CONTOUR NUMBER	CONTOUR LEVEL
1	-10500
2	-7000
3	-3500
4	0.00000000
5	3500

Figure 36 - S-Cage, Z-Normal Stress, Inertial Loading, Bridge Adjacent Large End

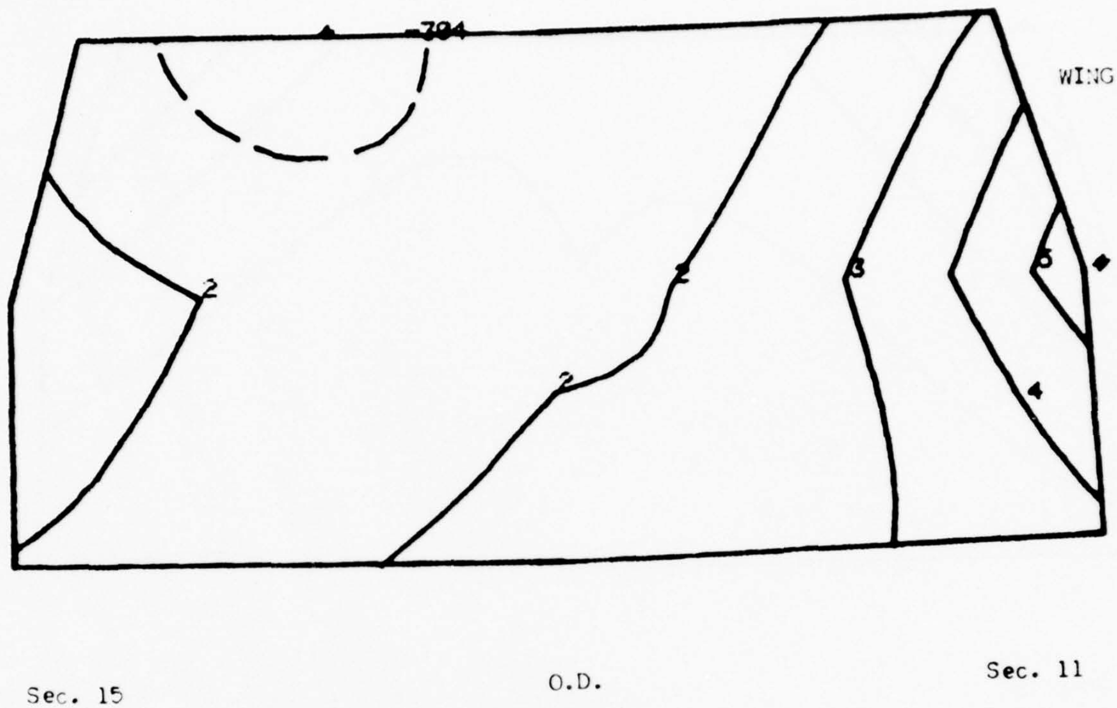

CONTOUR INTERVAL = 860 (psi)

CONTOUR NUMBER	CONTOUR LEVEL
1	0.00000000
2	860
3	1720
4	2580
5	3440

Figure 37 - S-Cage, X-Normal Stress, Inertial Loading Bridge Adjacent Small End

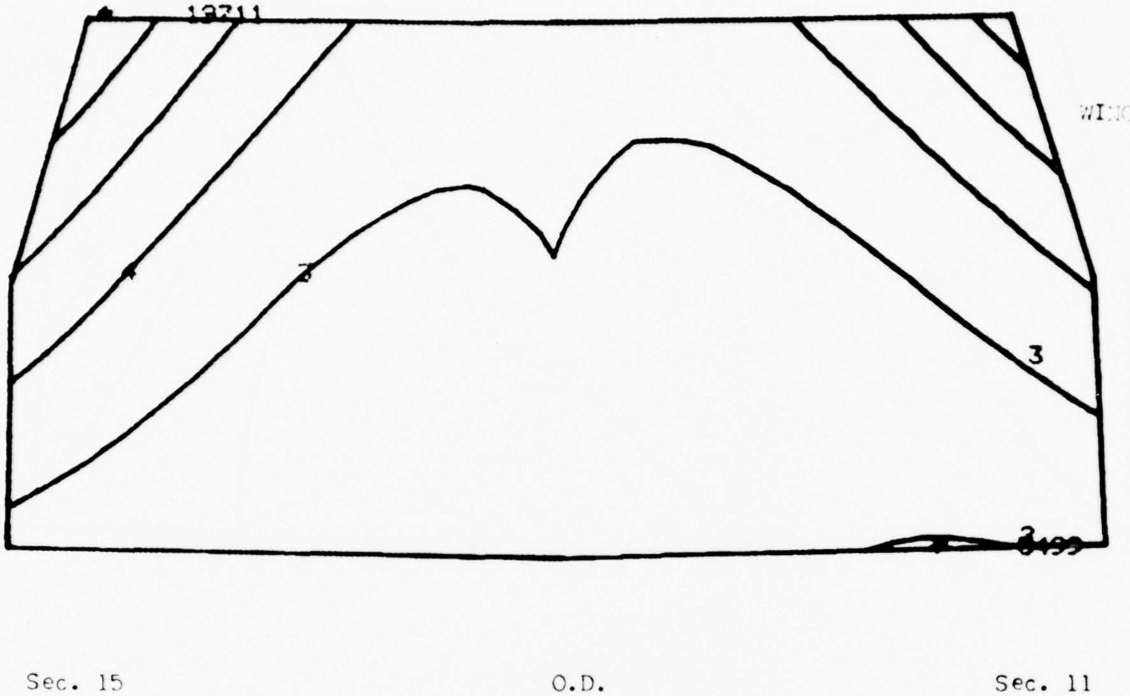

CONTOUR INTERVAL = 2800 (psi)

CONTOUR NUMBER	CONTOUR LEVEL
1	2800
2	5600
3	8400
4	11200
5	14000
6	16800
7	19600

Figure 38 - S-Cage, Y-Normal Stress, Inertial Loading, Bridge Adjacent Small End

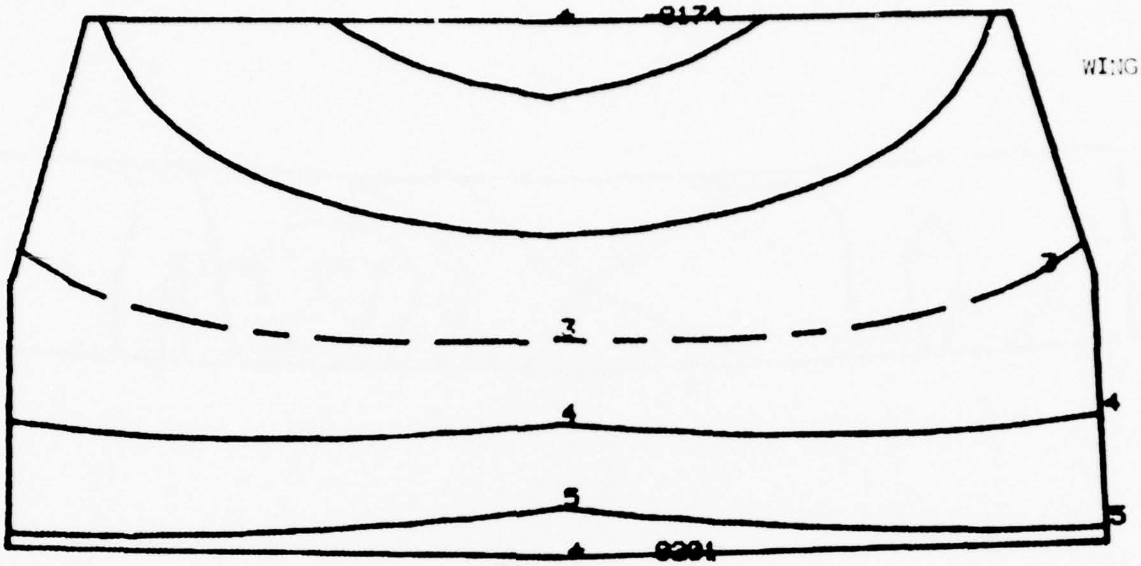

Sec. 15 O.D. Sec. 11

CONTOUR INTERVAL = 3200 (psi)

CONTOUR NUMBER	CONTOUR LEVEL
1	-6400
2	-3200
3	0.00000000
4	3200
5	6400

Figure 39 - S-Cage, Z-Normal Stress Inertial Loading Bridge Adjacent Small End

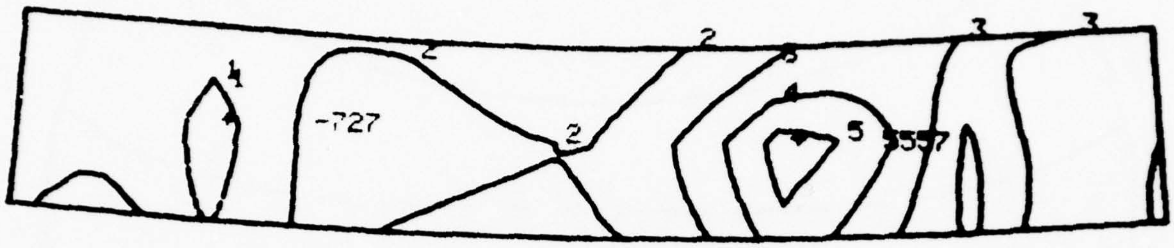

Sec. 7 O.D. Sec. 19

CONTOUR INTERVAL = 1250 (psi)

CONTOUR NUMBER	CONTOUR LEVEL
1	0.00000000
2	1250
3	2500
4	3750
5	5000

Figure 40 - S-Cage, X-Normal Stress Inertial Loading, Small End Adjacent Bridge

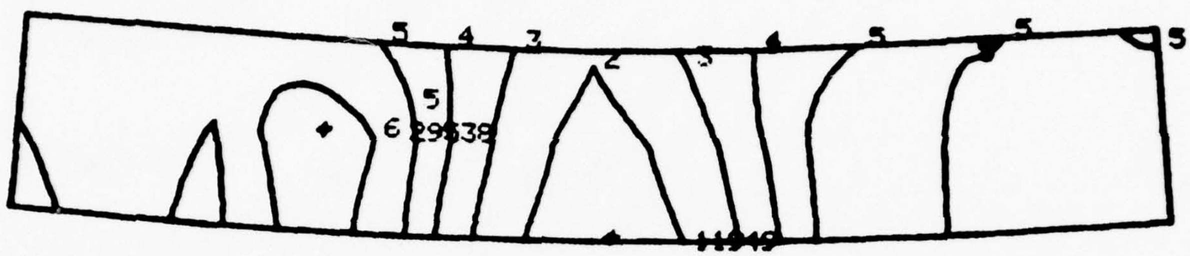

Sec. 7 O.D. Sec. 19

CONTOUR INTERVAL = 3500 (psi)

CONTOUR NUMBER	CONTOUR LEVEL
1	10500
2	14000
3	17500
4	21000
5	24500
6	28000

Figure 41 - S-Cage, Y-Normal Stress, Inertial Loading, Small End Adjacent Bridge

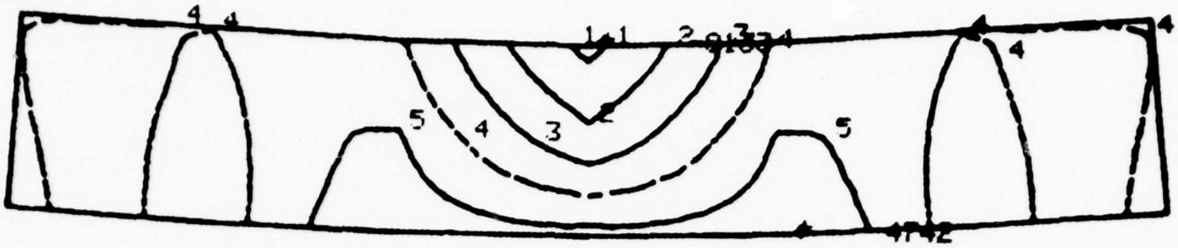

Sec. 7 O.D. Sec. 19

CONTOUR INTERVAL = 2500 (psi)

CONTOUR NUMBER	CONTOUR LEVEL
1	-7500
2	-5000
3	-2500
4	0.00000000
5	2500

Figure 42 - S-Cage, Z-Normal Stress Inertial Loading, Small End Adjacent Bridge

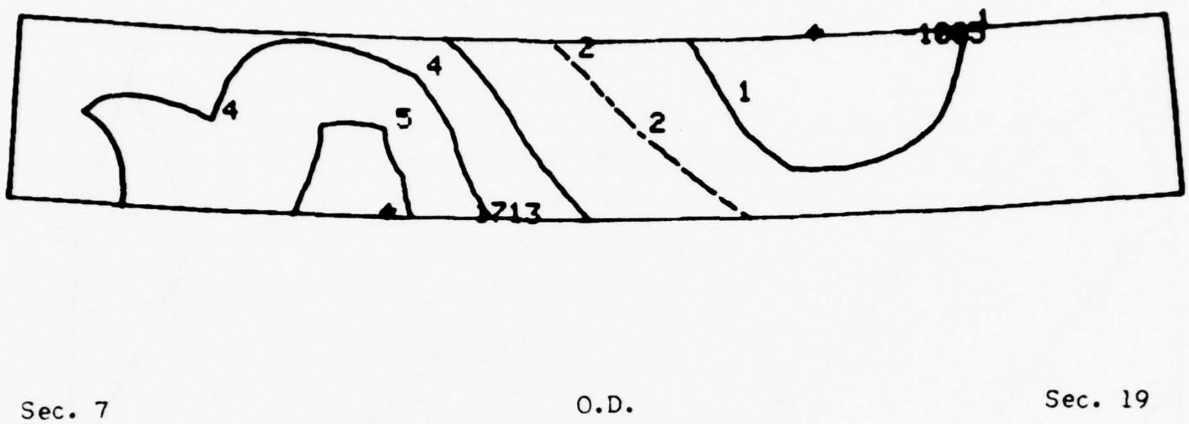

CONTOUR INTERVAL = 540 (psi)

CONTOUR NUMBER	CONTOUR LEVEL
1	-540
2	0.00000000
3	540
4	1080
5	1620

Figure 43 - S-Cage, Y-Normal Stress Bridge Loading, Large End Adjacent Bridge

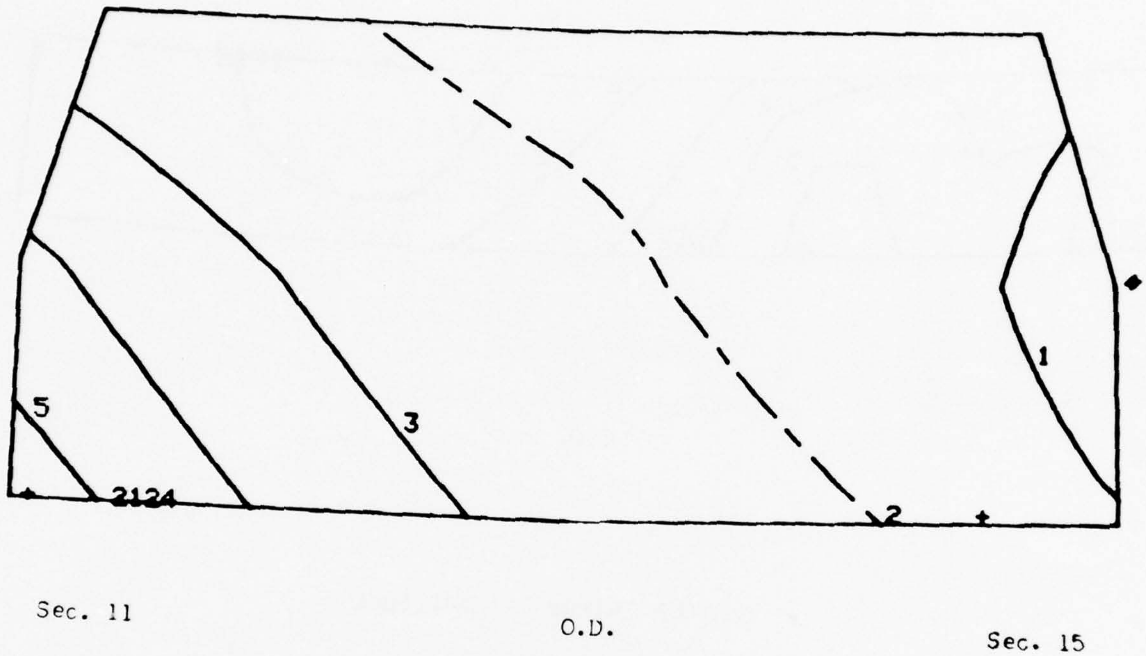

CONTOUR INTERVAL = 580 (psi)

CONTOUR NUMBER	CONTOUR LEVEL
1	-580
2	0.00000000
3	580
4	1160
5	1740

Figure 44 - S-Cage, Y-Normal Stress, Bridge Loading, Bridge Adjacent Large End

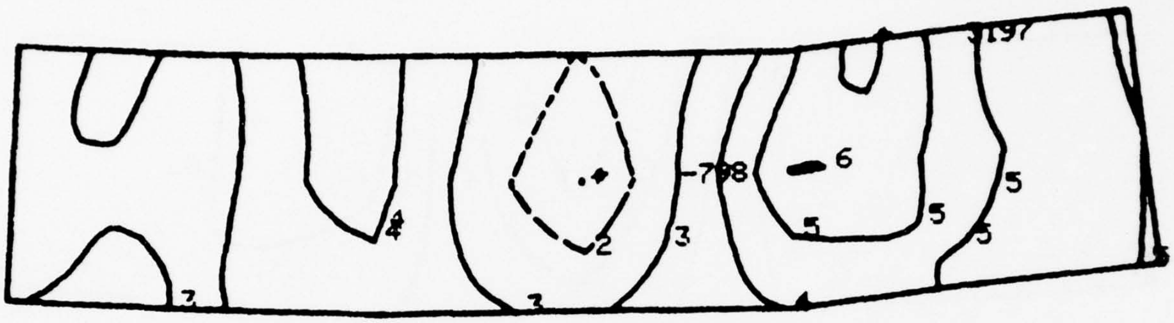

Sec. 7 O.D. Sec. 19

CONTOUR INTERVAL = 780 (psi)

CONTOUR NUMBER	CONTOUR LEVEL
1	-780
2	0.00000000
3	780
4	1560
5	2340
6	3120

Figure 45 - Z-Cage, X-Normal Stress, Inertial Loading, Large End Adjacent Bridge

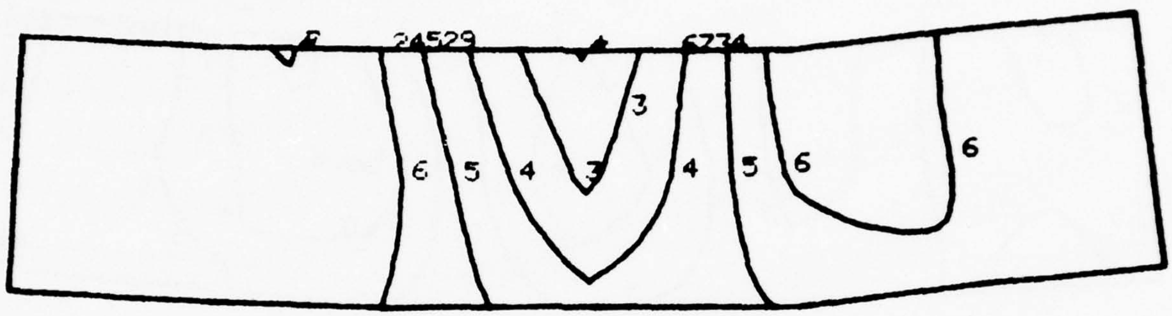

Sec. 7 O.D. Sec. 19

CONTOUR INTERVAL = 3500 (psi)

CONTOUR NUMBER	CONTOUR LEVEL
1	3500
2	7000
3	10500
4	14000
5	17500
6	21000
7	24500

Figure 46 - Z-Cage, Y-Normal Stress, Inertial Loading, Large End Adjacent Bridge

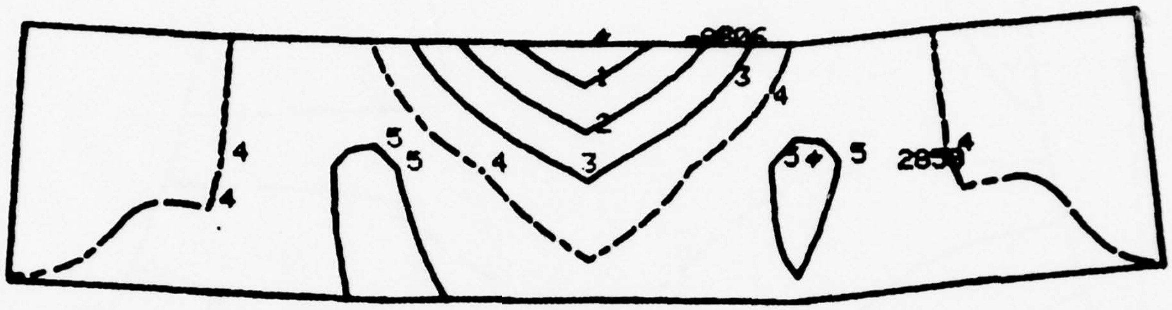

Sec. 7 O.D. Sec. 19

CONTOUR INTERVAL = 2200 (psi)

CONTOUR NUMBER	CONTOUR LEVEL
1	-6600
2	-4400
3	-2200
4	0.00000000
5	2200

Figure 47 - Z Cage, Z-Normal Stress, Inertial Loading, Large End Adjacent Bridge

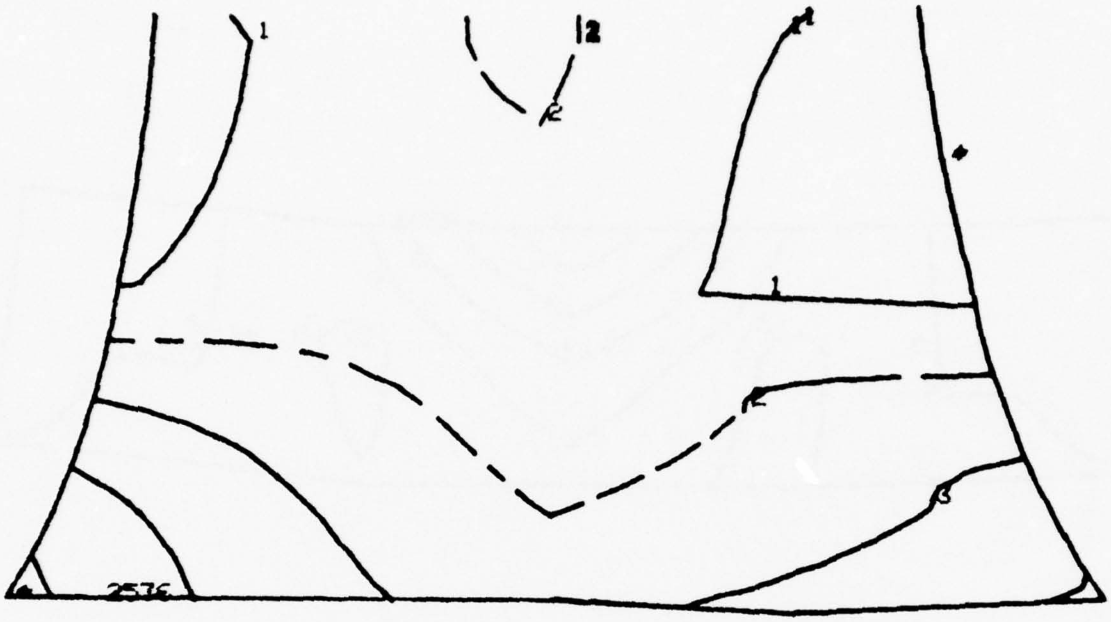

Sec. 11 O.D. Sec. 15

CONTOUR INTERVAL = 760 (psi)

CONTOUR NUMBER	CONTOUR LEVEL
1	-760
2	0.00000000
3	760
4	1520
5	2280

Figure 48 - Z-Cage, X-Normal Stress, Inertial Loading, Bridge Adjacent Large End

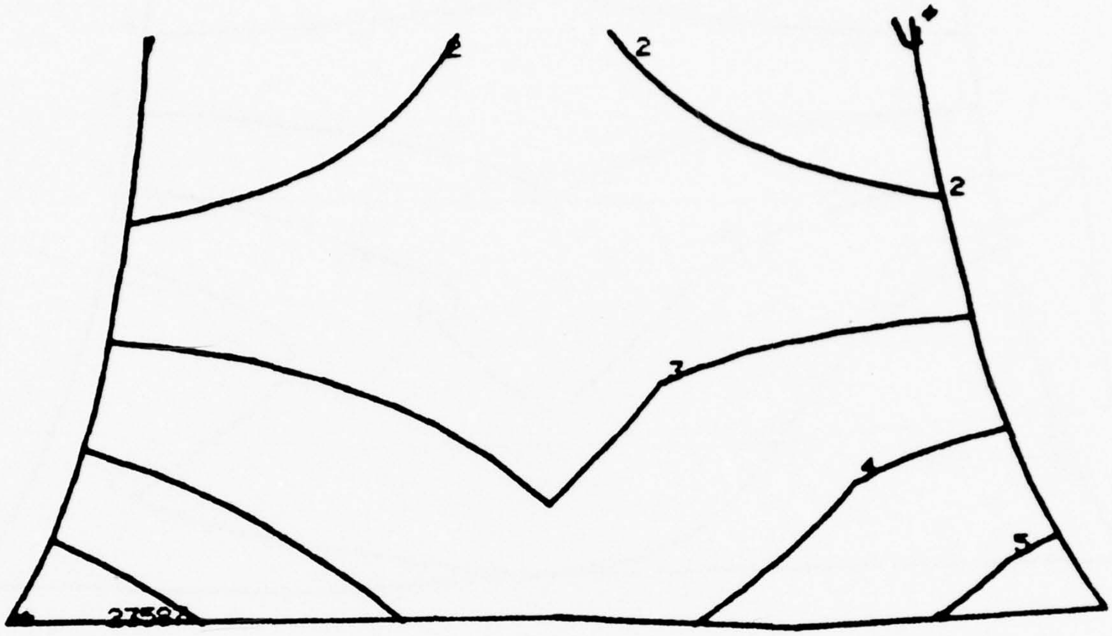

Sec. 11 O.D. Sec. 15

CONTOUR INTERVAL = 4600 (psi)

CONTOUR NUMBER	CONTOUR LEVEL
1	0.00000000
2	4600
3	9200
4	13800
5	18400
6	23000

Figure 49 - Z-Cage, Y-Normal Stress, Inertial Loading, Bridge Adjacent Large End

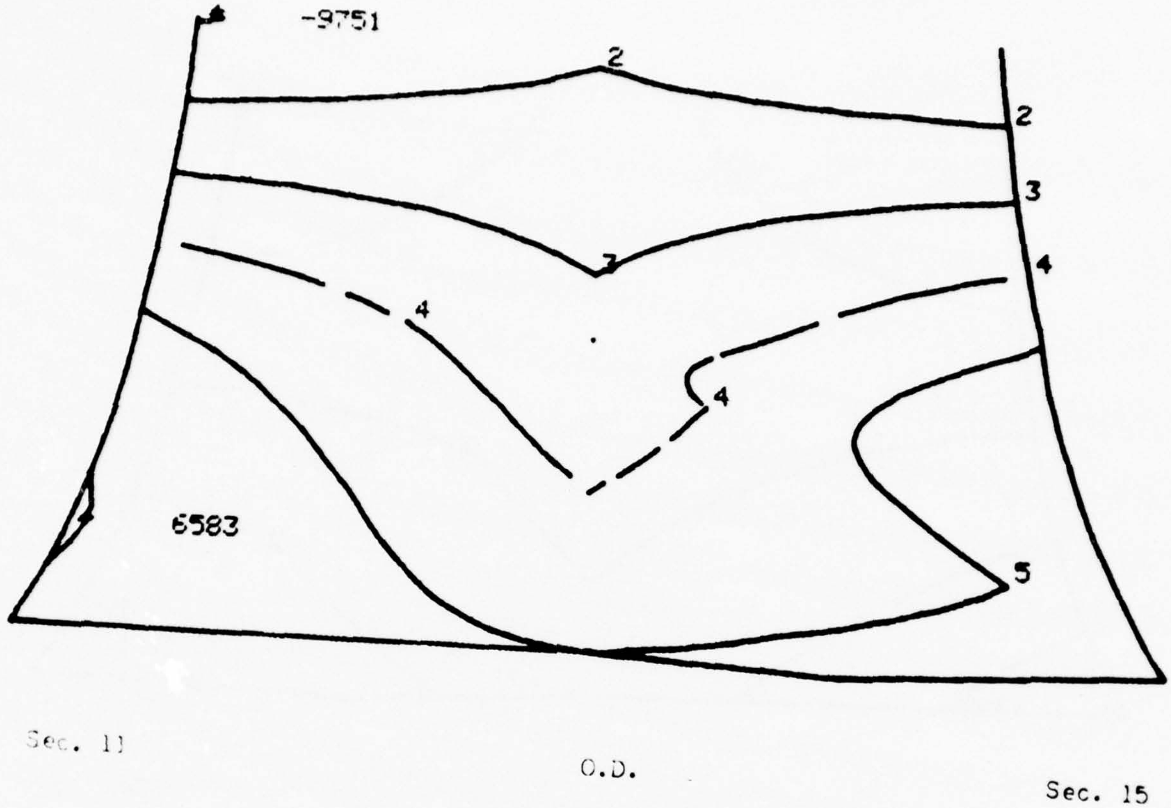

CONTOUR INTERVAL = 3200 (psi)

CONTOUR NUMBER	CONTOUR LEVEL
1	-9600
2	-6400
3	-3200
4	0.00000000
5	3200
6	6400

Figure 50 - Z-Cage, Z-Normal Stress, Inertial Loading, Bridge Adjacent Large End

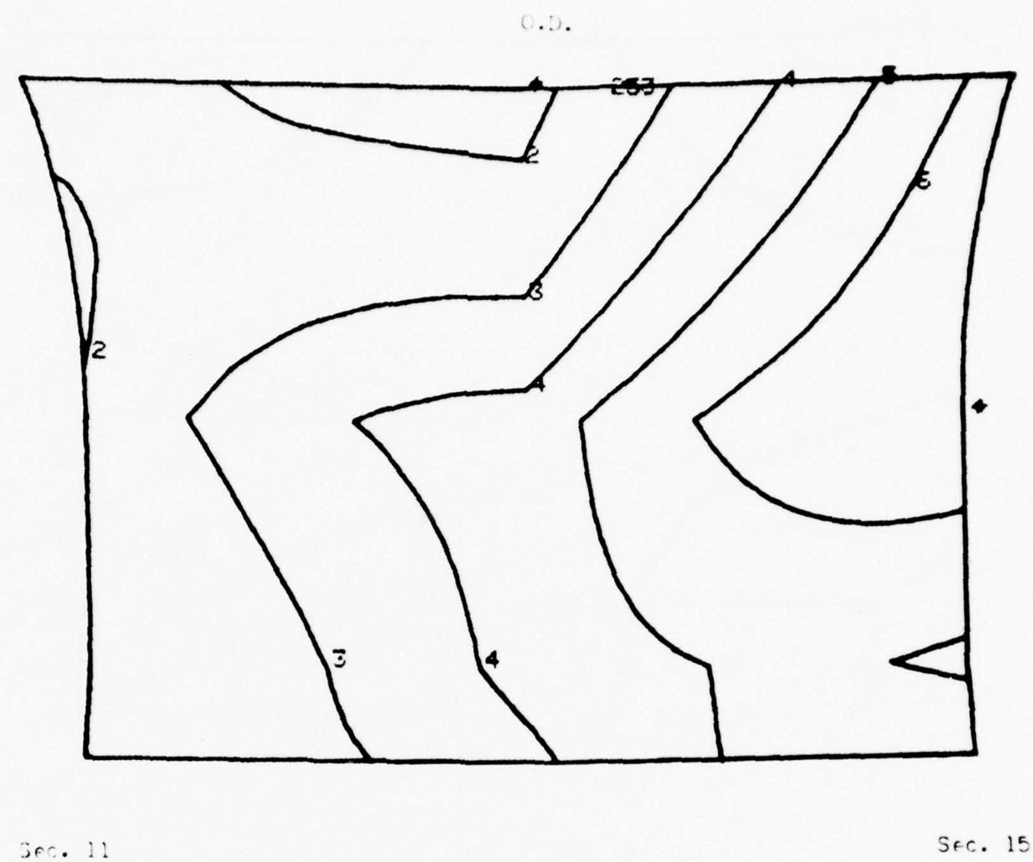

CONTOUR INTERVAL = 360 (psi)

CONTOUR NUMBER	CONTOUR LEVEL
1	0.00000000
2	360
3	720
4	1080
5	1440
6	1200

Figure 51 - Z-Cage, X-Normal Stress, Inertial Loading, Bridge Adjacent Small End

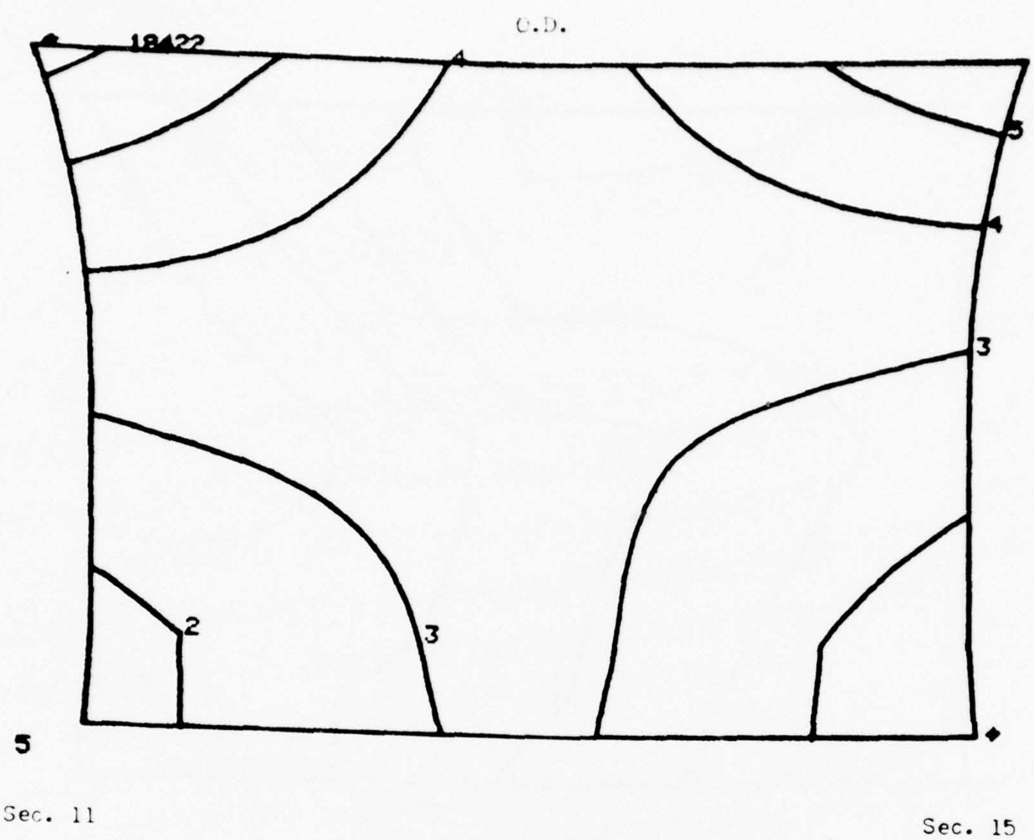

CONTOUR INTERVAL = 3400 (psi)

CONTOUR NUMBER	CONTOUR LEVEL
1	0.00000000
2	3400
3	6800
4	10200
5	13600
6	17000

Figure 52 - Z-Cage, Y-Normal Stress, Inertial Loading, Bridge Adjacent Small End

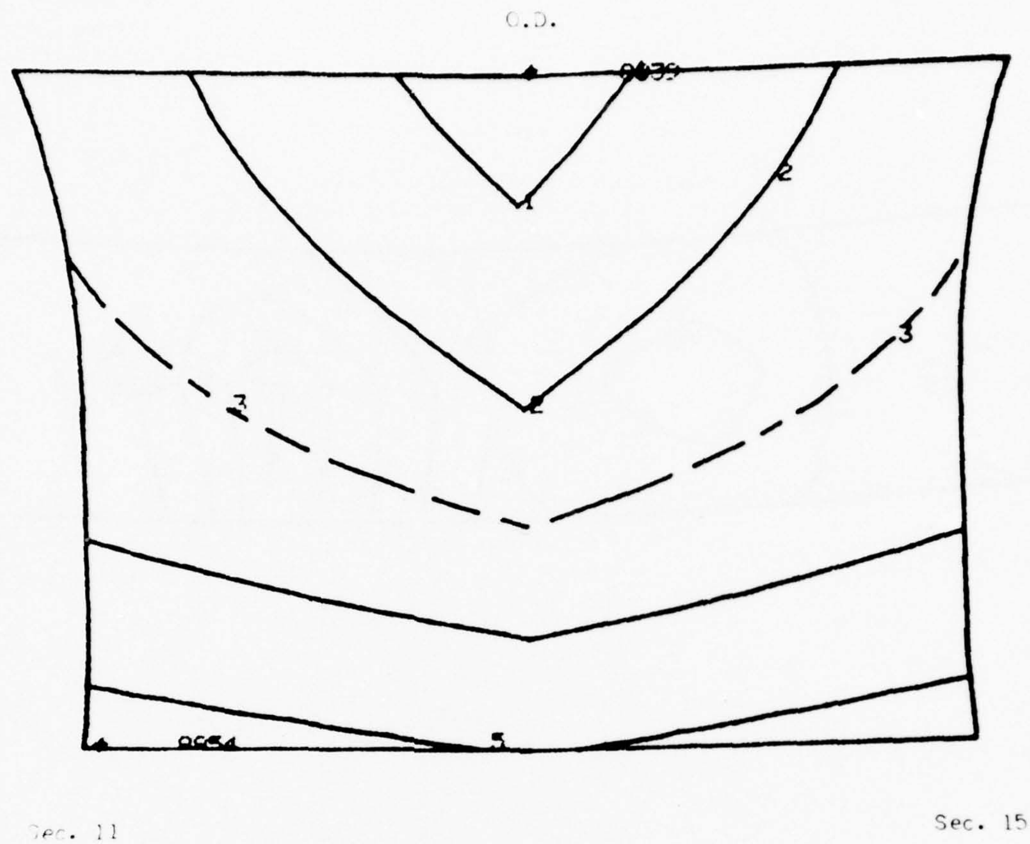

CONTOUR INTERVAL = 3500 (psi)

CONTOUR NUMBER	CONTOUR LEVEL
1	-7000
2	-3500
3	0.00000000
4	3500
5	7000

Figure 53 - Z-Cage, Z-Normal Stress, Inertial Loading, Bridge Adjacent Small End

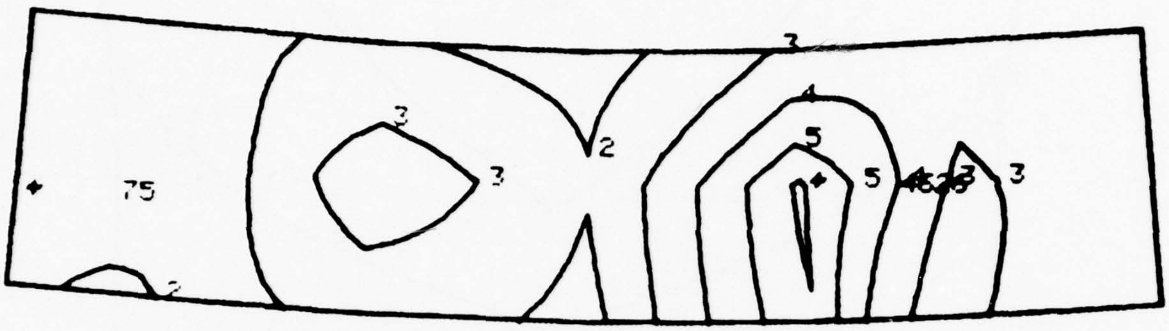

Sec. 7 O.D. Sec. 19

CONTOUR INTERVAL = 900 (psi)

CONTOUR NUMBER	CONTOUR LEVEL
1	0.00000000
2	900
3	1800
4	2700
5	3600
6	4500

Figure 54 - Z-Cage, X-Normal Stress, Inertial Loading, Small End Adjacent Bridge

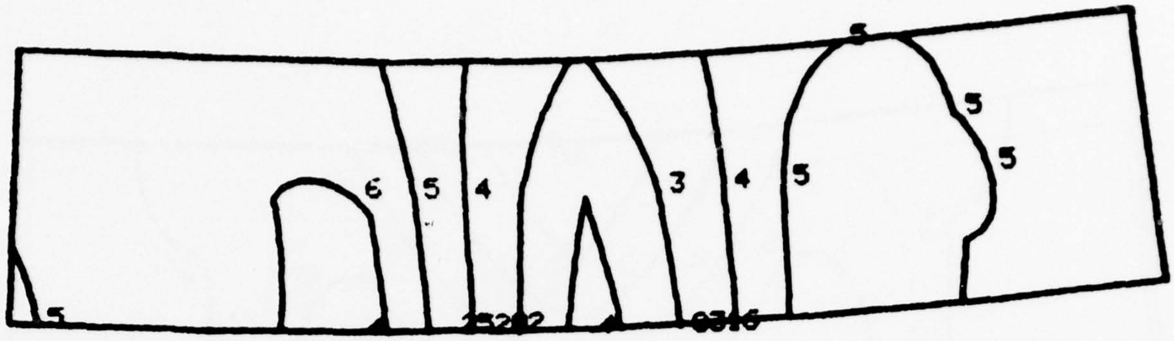

Sec. 7 O.D. Sec. 19

CONTOUR INTERVAL = 3300 (psi)

CONTOUR NUMBER	CONTOUR LEVEL
1	6600
2	9900
3	13200
4	16500
5	19800
6	23100

Figure 55 - Z-Cage, Y-Normal Stress Inertial Loading, Small End Adjacent Bridge

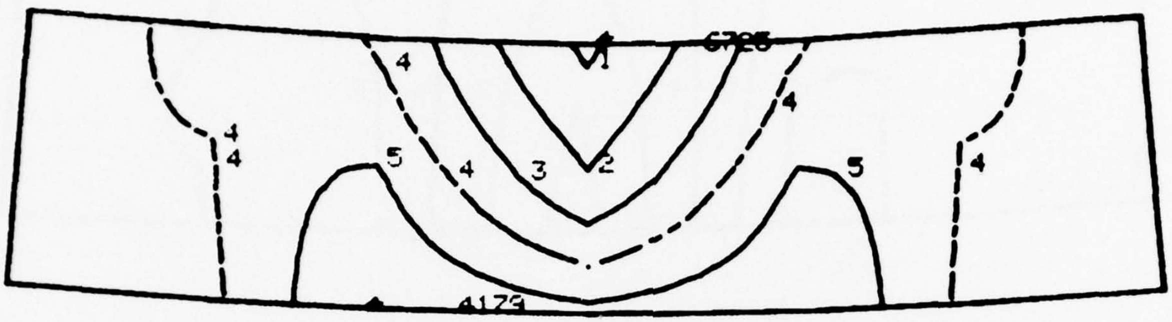

Sec. 7 O.D. Sec. 19

CONTOUR INTERVAL = 2100 (psi)

CONTOUR NUMBER	CONTOUR LEVEL
1	-6300
2	-4200
3	-2100
4	0.00000000
5	2100

Figure 56 - Z-Cage, Z-Normal Stress Inertial Loading, Small End Adjacent Bridge

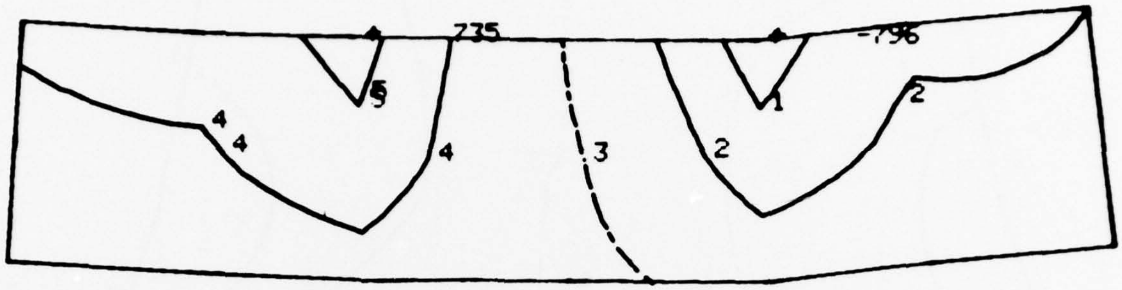

Sec. 7 O.D. Sec. 19

CONTOUR INTERVAL = 300 (psi)

CONTOUR NUMBER	CONTOUR LEVEL
1	-600
2	-300
3	0.00000000
4	300
5	600

Figure 57 - Z-Cage, Y-Normal Stress Bridge Loading, Large End Adjacent Bridge

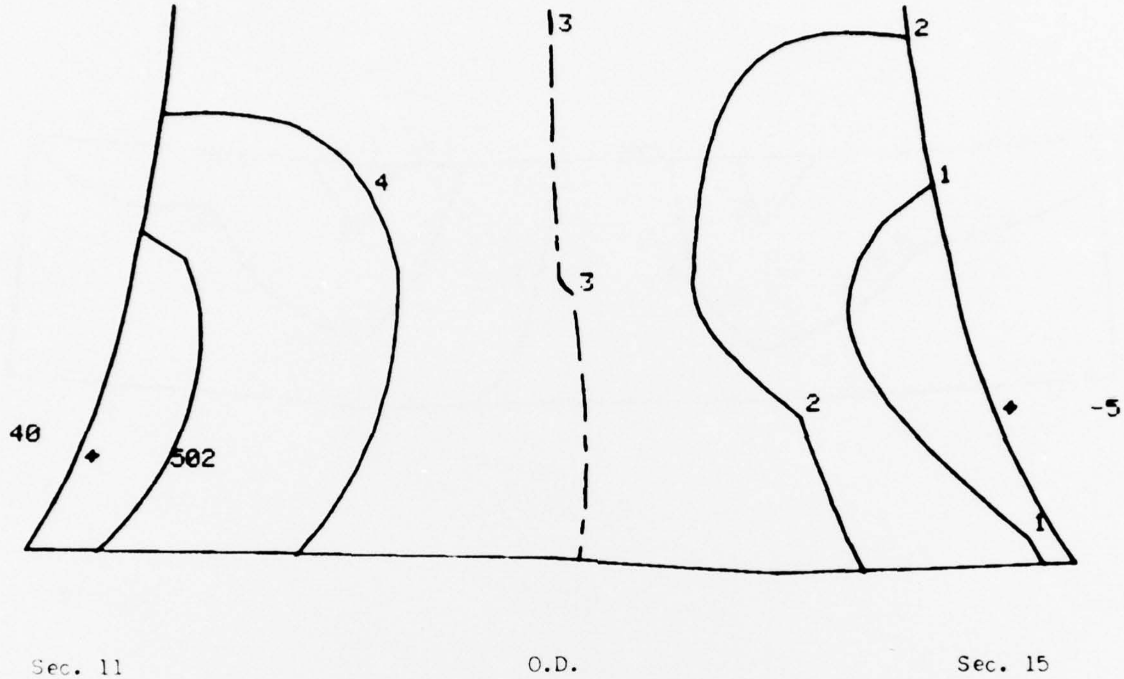

CONTOUR INTERVAL = 200 (psi)

CONTOUR NUMBER	CONTOUR LEVEL
1	-400
2	-200
3	0.00000000
4	200
5	400

Figure 58 - Z-Cage, Y-Normal Stress Bridge Loading, Bridge Adjacent Large End

TABLE 2

L-Cage

Maximum Stress and Deformation
For Solid Element Model-Inertial Loading

Section	* Position	Maximum U_x (In.)	* Location	Maximum σ_1 or σ_2 (PSI)	Location	Maximum Von Mises (PSI)	Location
7	SE	.00208	5	29,589	5	29,472	5
7	LE	.00251	10	34,990	9	35,140	9
8	SE	.00208	5	30,089	5	29,625	5
8	LE	.00251	10	34,390	9	34,316	9
9	SE	.00208	5	27,691	5	28,753	5
9	LE	.00252	10	33,758	9	34,211	9
10	SE	.00209	5	31,460	5	30,972	5
10	LE	.00252	10	36,404	9-10	34,729	9-10
11	SE	.00229	5	28,522	3-5	26,655	3-5
11	B	.00351	7-8	-30,728	7	30,656	7
11	LE	.00272	10	33,986	10-12	32,719	10-12
12	SE	.00229	5	21,687	1	22,110	3
12	B	.00349	7	-31,218	7	30,597	7
12	LE	.00272	10	26,207	12	26,205	12
13	SE	.00229	5	19,894	1	22,244	3
13	B	.00349	7	-31,711	7	30,542	7
13	LE	.00272	10	28,818	12	28,879	12
14	SE	.00229	5	21,687	1	22,111	3
14	B	.00349	7	-31,218	7	30,597	7
14	LE	.00272	10	26,204	12	26,202	12
15	SE	.00229	5	28,522	3-5	26,655	3-5
15	B	.00351	7-8	-30,728	7	30,656	7
15	LE	.00272	10	33,986	10-12	32,719	10-12
16	SE	.00209	5	31,460	5	30,972	5
16	LE	.00252	10	36,404	9-10	34,729	9-10
17	SE	.00208	5	27,691	5	28,753	5
17	LE	.00252	10	33,758	9	34,211	9
18	SE	.00208	5	30,089	5	29,625	5
18	LE	.00251	10	34,390	9	34,316	9
19	SE	.0208	5	29,590	5	29,472	5
19	LE	.0251	10	34,989	9	35,139	9

* See sketch in Figure 59 following tables. No.-No. indicates position midway between positions noted.

TABLE 3

L-Cage

Maximum Stress and Deformation
For Solid Element Model-Bridge Loading

Section	* Position	Maximum σ_1 or σ_2 (PSI)	Location	Maximum Von Mises (PSI)	Location
7	SE	1,258	5	1,552	3
7	LE	1,362	9	1,372	9
8	SE	1,377	5	1,615	3
8	LE	1,411	9-10	1,474	9-10
9	SE	1,473	3	1,796	3
9	LE	1,672	10	1,802	10
10	SE	2,139	5-6	2,101	5-6
10	LE	2,656	10	2,535	10
11	SE	2,755	3-4	2,341	3-4
11	B	-6,065	7	4,831	7
11	LE	3,101	10-12	2,941	10-12
12	SE	1,205	3-5	1,292	4
12	B	-4,043	8	3,656	7
12	LE	1,692	10-12	1,831	10-12
13	SE	936	4	1,316	4
13	B	2,788	8	2,899	8
13	LE	1,123	10	1,400	10
14	SE	919	4	1,270	4
14	B	3,737	8	3,797	8
14	LE	1,336	12	1,322	12
15	SE	-1,549	6	1,441	1
15	B	4,792	8	4,765	8
15	LE	1,669	12	1,655	12
16	SE	-1,252	5	1,203	5
16	LE	-1,647	9	1,588	9
17	SE	918	4	1,047	4
17	LE	1,430	12	1,437	12
18	SE	821	4	937	4
18	LE	1,189	12	1,271	10-12
19	SE	819	4	940	4
19	LE	1,085	10-12	1,283	10-12

* See sketch in Figure 59 following tables. No.-No. indicates position midway between positions noted.

TABLE 4

S-Cage

Maximum Stress and Deformation
For Solid Element Model-Inertial Loading

Section	* Position	Maximum U_x (In.)	* Location	Maximum σ_1 or σ_2 (PSI)	Location	Maximum Von Mises (PSI)	Location
7	SE	.00208	5	29,571	5	29,461	5
7	LE	.00236	6	29,319	9	29,388	9
8	SE	.00208	5	30,084	5	29,628	5
8	LE	.00235	10	30,052	9-10	29,700	9-10
9	SE	.00208	5	27,747	5	28,800	5
9	LE	.00236	10	29,580	9	30,056	9
10	SE	.00208	5	32,582	5-6	31,063	5
10	LE	.00235	10	34,100	9-10	32,477	10
11	SE	.00207	5	28,652	5-6	26,763	5-6
11	B	.00344	7-8	-31,264	7	31,188	7
11	LE	.00236	10	32,189	10	30,404	10
12	SE	.00207	5	21,801	1	22,209	3-5
12	B	.00342	7-8	-31,763	7	31,132	7
12	LE	.00237	10	22,464	10-12	23,794	9-11
13	SE	.00207	5	20,005	1	21,664	3-5
13	B	.00342	7-8	-32,266	7	31,080	7
13	LE	.00236	10	21,477	11	24,409	9-11
14	SE	.00207	5	21,801	1	22,209	3-5
14	B	.00342	7-8	-31,763	7	31,132	7
14	LE	.00237	10	22,464	10-12	23,794	9-11
15	SE	.00207	5	28,652	5-6	26,763	5-6
15	B	.00344	7-8	-31,264	7	31,188	7
15	LE	.00236	10	32,189	10	30,404	10
16	SE	.00208	5	32,582	5-6	31,063	5
16	LE	.00235	10	34,100	9-10	32,477	10
17	SE	.00208	5	27,747	5	28,800	5
17	LE	.00236	10	29,580	9	30,056	9
18	SE	.00208	5	30,084	5	29,628	5
18	LE	.00235	10	30,052	9-10	29,700	9-10
19	SE	.00208	5	29,571	5	29,461	5
19	LE	.00236	6	29,319	9	29,388	9

* *See sketch in Figure 59 following tables.* No.-No. indicates position midway between positions noted.

TABLE 5

S-Cage

Maximum Stress and Deformation
For Solid Element Model-Bridge Loading

Section	* Position	Maximum σ_1 or σ_2 (PSI)	Location	Maximum Von Mises (PSI)	Location
7	SE	1,177	5	1,340	3
7	LE	1,106	9-10	1,195	9-10
8	SE	1,281	5	1,388	3
8	LE	1,265	10	1,322	9-10
9	SE	1,295	3-5	1,544	3
9	LE	1,438	10	1,569	10
10	SE	1,981	5-6	1,939	5-6
10	LE	2,216	10	2,109	10
11	SE	2,570	5-6	2,193	5-6
11	B	-6,010	7	4,782	7
11	LE	2,543	10	2,365	10
12	SE	1,008	5	1,184	6
12	B	-4,019	7	3,635	7
12	LE	1,285	10	1,400	10
13	SE	866	4	1,173	4
13	B	2,748	8	2,855	8
13	LE	694	13	1,046	12
14	SE	845	3	1,104	4-6
14	B	3,660	8	3,718	8
14	LE	- 803	10-12	995	10-12
15	SE	-1,439	5-6	1,281	4-6
15	B	4,672	8	4,645	8
15	LE	-1,519	9-10	1,382	10
16	SE	-1,166	5	1,120	5
16	LE	962	14	952	14
17	SE	859	4	1,014	4
17	LE	897	14	965	12
18	SE	764	4	904	4
18	LE	756	14	911	12
19	SE	763	4	917	4
19	LE	661	13-14	961	12

* See sketch in Figure 59 following tables. No.-No. indicates position midway between positions noted.

TABLE 6

Z-Cage

Maximum Stress and Deformation
For Solid Element Model-Inertial Loading

Section	* Position	Maximum U_x (In.)	* Location	Maximum σ_1 or σ_2 (PSI)	Location	Maximum Von Mises (PSI)	Location
7	SE	.00172	5	23,032	5	23,420	5
7	LE	.00186	10	23,237	9	24,151	9
8	SE	.00172	5	23,212	5	23,522	5
8	LE	.00186	10	24,128	9	24,229	9
9	SE	.00173	5	24,268	5	24,349	5
9	LE	.00186	10	23,935	9-10	24,856	9-10
10	SE	.00173	5	26,472	5-6	25,048	5-6
10	LE	.00186	10	27,635	9-10	26,320	9-10
11	SE	.00173	5	28,591	6	27,403	6
11	B	.00238	7-8	-21,057	7	21,064	7
11	LE	.00186	10	29,705	10	28,343	10
12	SE	.00173	5	18,557	3-5	20,205	3-5
12	B	.00237	7-8	-20,909	7	20,867	7
12	LE	.00187	10	19,031	10-12	19,843	9-11
13	SE	.00172	5	18,774	3-5	21,735	3-5
13	B	.00236	8	-20,761	7	20,670	7
13	LE	.00188	10	19,891	10-12	21,177	9-11
14	SE	.00173	5	18,557	3-5	20,205	3-5
14	B	.00237	7-8	-20,909	7	20,867	7
14	LE	.00187	10	19,031	10-12	19,843	9-11
15	SE	.00173	5	28,591	6	27,403	6
15	B	.00238	7-8	-21,057	7	21,064	7
15	LE	.00186	10	29,705	10	28,343	10
16	SE	.00173	5	26,472	5-6	25,048	5-6
16	LE	.00186	10	27,635	9-10	26,320	9-10
17	SE	.00173	5	24,268	5	24,349	5
17	LE	.00186	10	23,935	9-10	24,856	9-10
18	SE	.00172	5	23,212	5	23,522	5
18	LE	.00186	10	24,128	9	24,229	9
19	SE	.00172	5	23,032	5	23,420	5
19	LE	.00186	10	23,237	9	24,151	9

* See sketch in Figure 59 following tables. No.-No. indicates position midway between positions noted.

TABLE 7

Z-Cage

Maximum Stress and Deformation
For Solid Element Model-Bridge Loading

Section	* Position	Maximum σ_1 or σ_2 (PSI)	Location	Maximum Von Mises (PSI)	Location
7	SE	274	5	275	5
7	LE	361	9	379	9
8	SE	295	5	306	5
8	LE	423	9	414	9
9	SE	339	4-6	366	6
9	LE	448	11	469	9
10	SE	535	5-6	508	5-6
10	LE	588	9	581	9
11	SE	955	5	819	5
11	B	-2,920	7-8	2,120	8
11	LE	1,063	9-10	862	9-10
12	SE	435	4-6	397	4-6
12	B	-1,614	7-8	1,225	7-8
12	LE	452	9-10	398	9-10
13	SE	- 261	4-6	436	4-6
13	B	- 513	5-7	811	8-10
13	LE	245	10-12	419	10-12
14	SE	- 525	5-6	455	5-6
14	B	916	8	990	8
14	LE	- 447	9-10	408	9
15	SE	-1,197	5-6	986	5-6
15	B	1,739	8	1,697	8
15	LE	-1,073	9	909	9
16	SE	- 503	5-6	480	6
16	LE	- 609	9	591	9
17	SE	- 305	5	340	5
17	LE	- 432	9-11	449	9
18	SE	- 271	5	281	5
18	LE	- 402	9	394	9
19	SE	- 248	5	249	5
19	LE	- 341	9	357	9

* See sketch in Figure 59 following tables. No.-No. indicates position midway between positions noted.

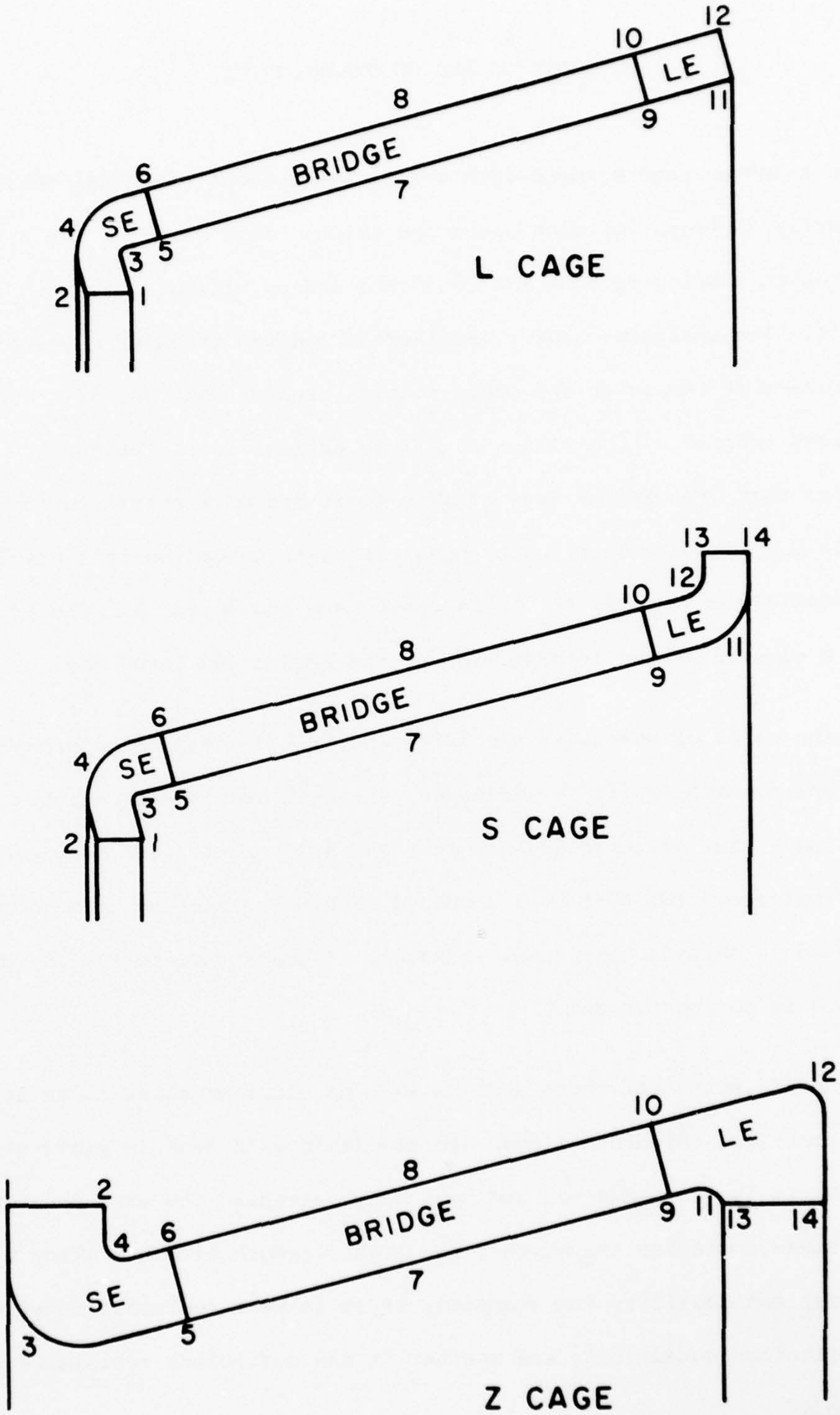

Figure 59 - Cage Cross-Sectional Grids to Locate Maximum Stresses and Deformation

SECTION V

CONCLUSIONS AND RECOMMENDATIONS

The L-design cage stamped from a low carbon sheet steel has inadequate tensile strength for high speed operation. This material has a tensile yield strength ranging from 30 KSI to 36 KSI and an ultimate strength in the low 40's. The analysis considering inertia induced stresses revealed tensile stresses at the large end cross-section greater than 36 KSI. The additional stress induced by the roller-cage interaction clearly produces a stress level that exceeds the cage elastic limit and will result in fracture. This has been demonstrated by physical tests conducted in a previous investigation. (ref. 1) These tests have indicated that the critical region of a cage is at the intersection of the bridge and large end.

On the basis of stress at the large end, the S-design cage produced by stamping, affords little additional strength over the L-design. Manufacturing either of these designs from SAE 4340 steel (tensile yield approximately 100 KSI) by a combined machining/stamping technique could provide a satisfactory cage. However, if cracks are formed in manufacture, there is no improvement.

Producing either of these designs with an aluminum alloy is an attractive alternative. Aluminum alloys are available with tensile yield strengths equal to low carbon steel and have only one-third the mass density. Possible obstacles are whether the high strength aluminum alloy has sufficient ductility for stamping, if it is wear resistant under marginal lubrication conditions, and whether it has sufficient resistance to creep.

Structurally, the Z cage is the superior design. It has the greatest resistance to inertia induced forces (lowest stress level) and exhibits minimum deformation. Stresses produced by roller-cage interaction have the least effect on this design. Disadvantages of this design are its complexity of manufacture and its additional heat generation (to be investigated in TASK III).

Recommendations

The economics and other possible disadvantages of the machined Z cage justify further development of a homogenous, isotropic L or S-design cage of increased tensile strength. In conjunction with this activity, developmental efforts (TASK II) should also concentrate on producing the L-design with a high strength, wear resistant aluminum alloy. However, unless there are positive results from these activities, the machined Z cage should be used in the bearing endurance tests (TASK IV). This would be contingent on the results of the bearing performance tests (TASK III).

REFERENCES

1. Cornish, R. F., Orvos, P. S., and Dressler, G. J., "Design, Development and Testing of High Speed Tapered Roller Bearings for Turbine Engines," Technical Report AFAPL-TR-75-26, The Timken Company, July 1975.

2. Boness, R. J., "The Effect of Oil Supply on Cage and Roller Motion in a Lubricated Roller Bearing," Journal of Lubrication Technology, Transactions of ASME, Series F, Vol. 92, No. 1, Jan. 1970, pp. 39-53.

3. Poplawski, J. V., and Mauriello, J. A., "Skidding in Lightly Loaded High-Speed Ball Thrust Bearings," ASME Paper 69-Lub-20, Lubrication Symposium, San Francisco, California, June 17-19, 1969.

4. Harris, T. A., "An Analytical Method to Predict Skidding in Thrust-Loaded Angular-Contact Ball Bearings," Journal of Lubrication Technology, Transactions of ASME, Series F, Vol. 93, No. 1, Jan. 1971, pp. 17-25.

5. Walters, C. T., "The Dynamics of Ball Bearings," Journal of Lubrication Technology, Transactions of ASME, Series F, Vol. 93, No. 1, Jan. 1971, pp. 1-11.

6. Poplawski, J. V., "Slip and Cage Forces in a High Speed Roller Bearing," Journal of Lubrication Technology, Transactions of ASME, Series F, No. 2, Apr. 1972, pp. 143-153.

7. Gupta, P. K., "Analysis of Cage Motion," Technical Report AFAPL-TR-76-28, Mechanical Technology, Incorporated, Feb. 1976.

8. "Mechanical Design Library Part IV," Structural Dynamics Research Corporation, 1976.

9. Huang, Y., "Finite Element Method - Structure Analysis by Simulation," Presented at the SAE Earthmoving Industry Conference, Peoria, Illinois, Apr. 2-4, 1973.

10. Mauriello, J. A., et al, "Rolling Element Bearing Retainer Analyses," USAAMRDL Technical Report 72-45, Nov. 1973.

APPENDIX

Section Properties for Beam Elements

Units - Inches, Degrees

Cage Design	Cross Section	Area $(\cdot 10^2)$	Principal Axis Area $Y(\cdot 10^5)$	Principal Axis Moments $Z(\cdot 10^5)$	Shear Area Ratio Y	Shear Area Ratio Z	Torsional Constant $(\cdot 10^5)$	Eccentricity ey	Eccentricity ez	Rotation Angle
L	Small End	1.008	1.535	.5147	1.159	1.295	1.161	.011	-.003	53.772
L	Large End	.709	.249	.701	1.118	1.048	.708	0	0	103.0
L	Bridge	.831	.271	1.216	1.134	1.091	.844	.001	.003	0
L	Large End (Extended)	1.115	.395	2.732	1.118	1.048	.708	0	0	103.0
S	Large End	1.087	2.147	.497	1.189	1.242	1.279	-.010	0	54.089
Z	Small End	2.609	9.193	3.596	1.178	1.229	8.445	.012	.004	153.485
Z	Large End	1.924	5.322	1.73	1.153	1.122	4.941	-.004	.001	168.16
Z	Bridge	1.099	.724	1.399	1.141	1.141	1.714	0	0	0

☆ U. S. GOVERNMENT PRINTING OFFICE: 1977 — 757-001/449